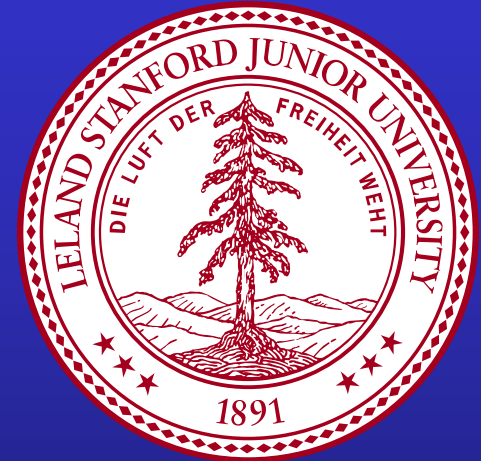
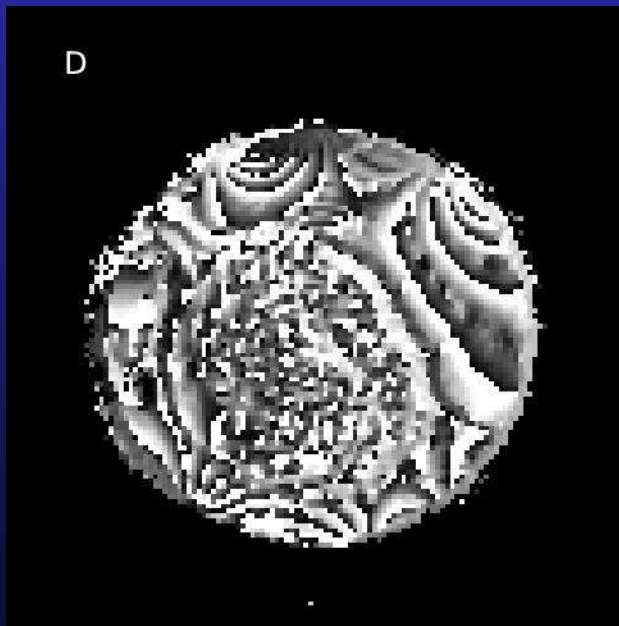
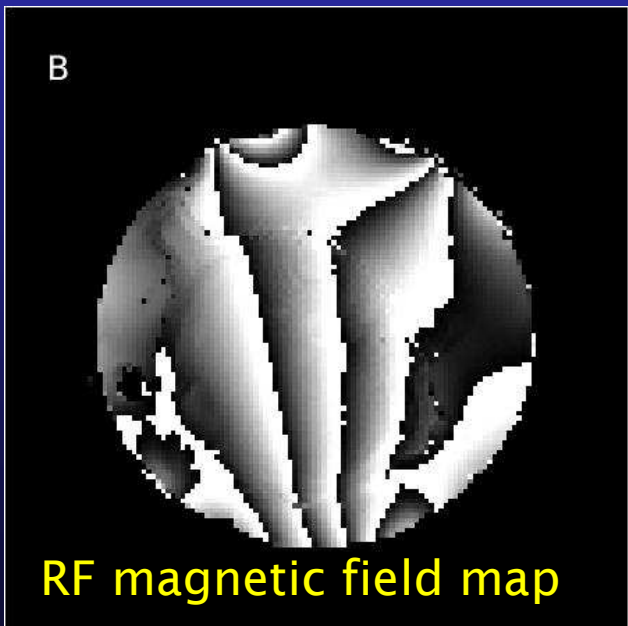
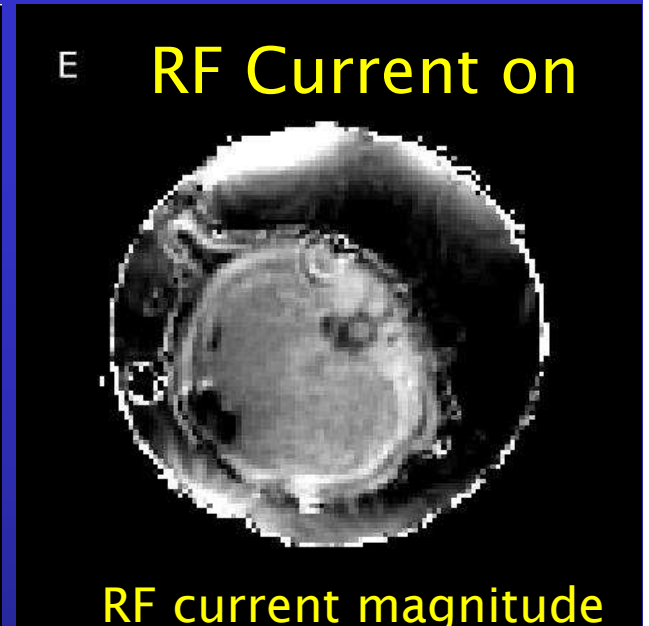
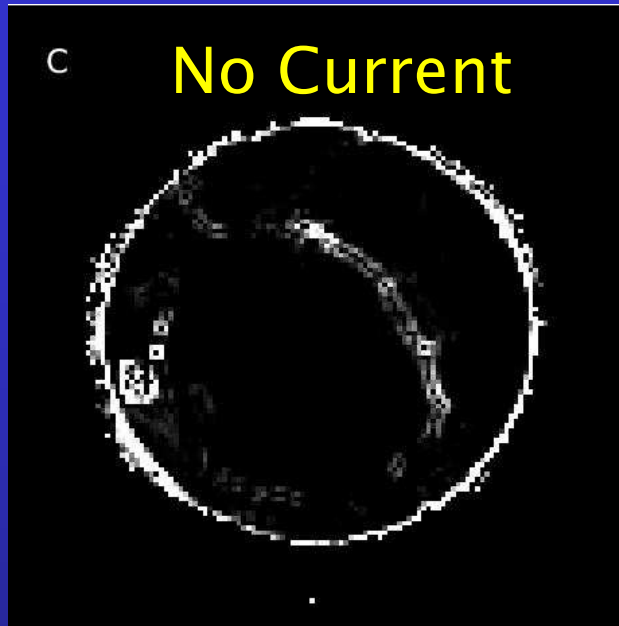
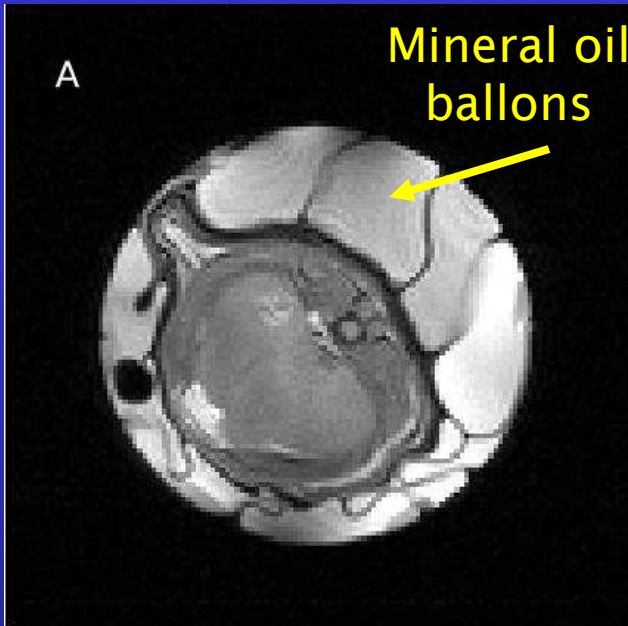


The Physical Basis of RF Electrical Properties Contrast Imaging by MRI



Greig Scott

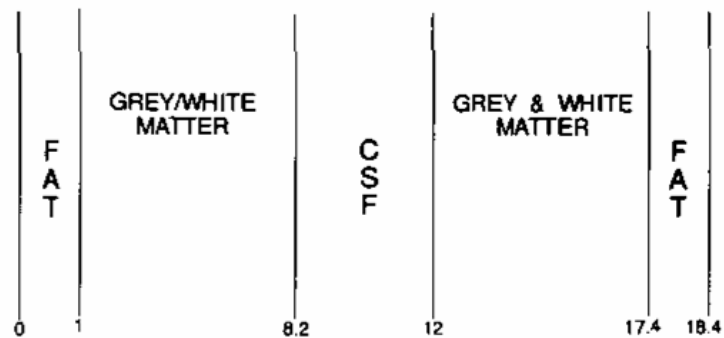
Department of Electrical Engineering
Stanford University



Rat – Post Mortem: 2T, 86.6 MHz (1993)

Extraction of conductivity and permittivity using magnetic resonance imaging

E M Haacke†‡, L S Petropoulos†, E W Nilges† and D H Wu§



Tissue	$\sigma \pm \Delta\sigma$ $S m^{-1}$	$\epsilon \pm \Delta\epsilon$	Noise (%)
White/Grey matter	0.303 ± 0.002	100.700 ± 0.449	1
	0.312 ± 0.008	98.939 ± 0.429	3
	0.329 ± 0.023	102.444 ± 2.045	5
CSF	1.504 ± 0.016	62.187 ± 0.608	1
	1.479 ± 0.070	63.720 ± 3.653	3
	1.496 ± 0.133	76.083 ± 3.280	5
White/Grey matter	0.291 ± 0.002	98.461 ± 0.405	1
	0.285 ± 0.005	96.321 ± 1.098	3
	0.278 ± 0.012	94.363 ± 1.961	5

Suggested processing 2nd derivatives of RF field, but field & phase stability were inadequate at the time: impractical.

Feasibility of RF Current Density Imaging

G.C. Scott* M.L.G. Joy* R.L. Armstrong† R.M. Henkelman‡

*Dept. Elec. Eng., Inst. Biomed. Eng., †Dept. of Physics, ‡Dept. of Medical Biophysics
University of Toronto, Toronto, Ontario, CANADA

1 Introduction

In past work, our group has shown that MRI can image quasistatic volume current densities in electrolytic and biological media (1), (2), (3). We wish to extend the method to image RF current density at the Larmor frequency. RF current imaging would be relevant to MR power absorption and to hyperthermia analysis. The approach is to deliberately induce or inject RF currents in the sample synchronous with an MR pulse sequence and measure the resulting RF magnetic fields in 3 dimensions by MRI. Curl, divergence and vector Laplacian operations on the magnetic fields respectively give current density, check data consistency and yield material information. In this report, the feasibility of injecting an RF current into an electrolyte sample and detecting its magnetic field by MRI is studied.

- 1) Inject RF current at Larmor frequency.
- 2) B1 field maps. How???
- 3) Curl the field maps.
- 4) Multiple cycles needed for high SNR.

We had a 2T animal spectroscopy system with two transmitter channels for homo/hetero nuclear decoupling.

Field Equation Overview

$$\nabla^2 \vec{H} = j\omega\mu(\sigma + j\omega\epsilon)\vec{H} + \vec{J} \times \frac{\nabla(\sigma + j\omega\epsilon)}{(\sigma + j\omega\epsilon)}$$

Wave eqn

$$\nabla^2 \vec{H} = \nabla(\sigma + j\omega\epsilon) \times \nabla V$$

Poisson/Laplace

MRI: B_+ : Transmit, B_- : receive

$$\vec{B}_L = (B_x - jB_y)(\hat{x} + j\hat{y})/2 \rightarrow B_+$$

$$\vec{B}_R = (B_x + jB_y)(\hat{x} - j\hat{y})/2 \rightarrow B_-$$

$$\vec{B}_Z = B_o \hat{z}$$

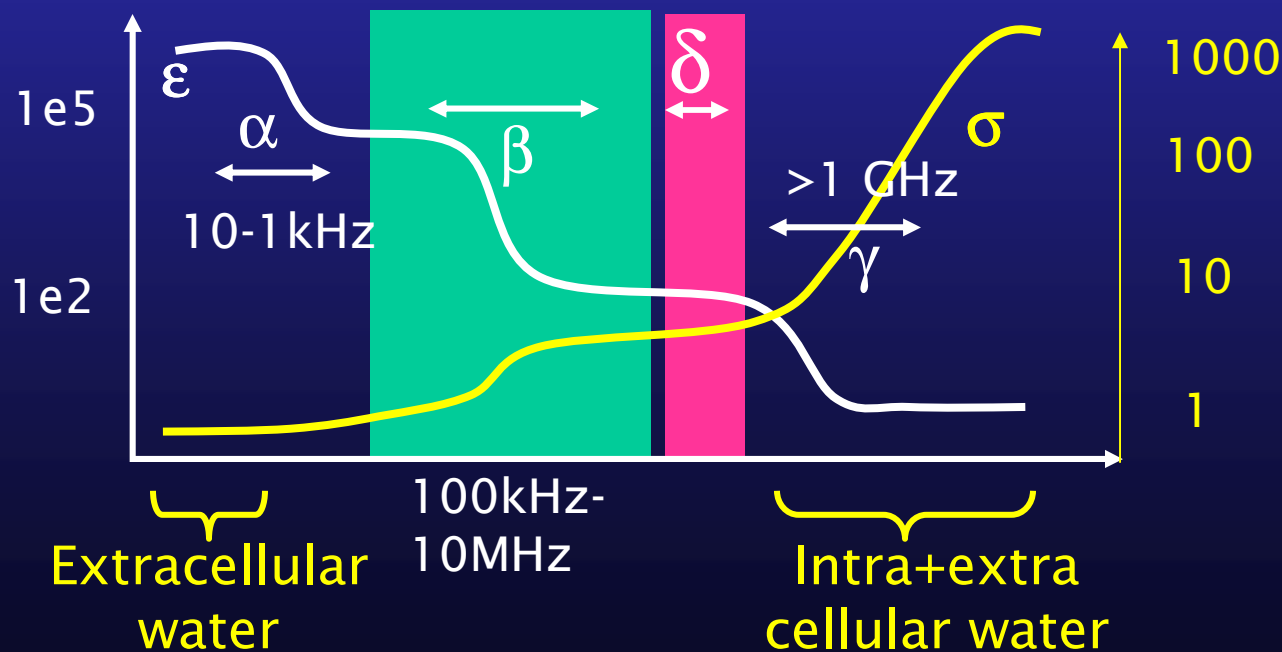
$$I = f(B_+) B_-$$

Image

$$\text{Re}[B_+ e^{j\omega t}] \quad \vec{B} = \mu_o \vec{H}$$

Tissue Impedance Biophysics

- α dispersion: cell membrane-electrolyte surface effect.
- β dispersion: capacitive charging of cell membranes, dipolar reorientation of proteins, organelles.
- δ dispersion: protein suspension in water $\sim 100\text{MHz}$.
- γ dispersion: polar properties of free water.



Challenges

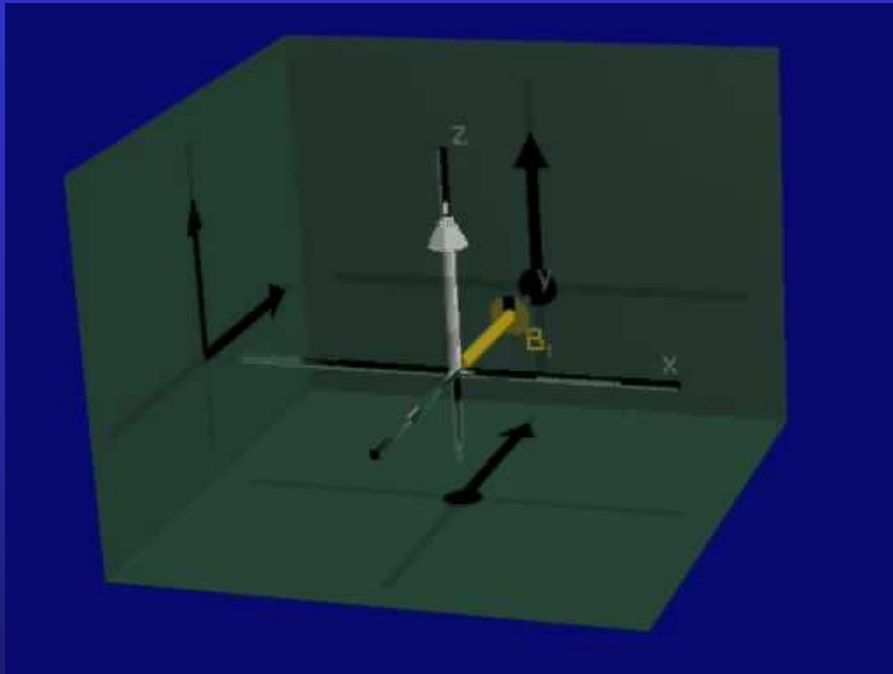
- Converting MRI B maps to lab frame H.
- B1 Mapping with high dynamic range.
- Inverse problem to compute missing components.
- Vector Field Tomography.

Transmit Sensitivity

$$B_+ = (B_x - jB_y)/2$$

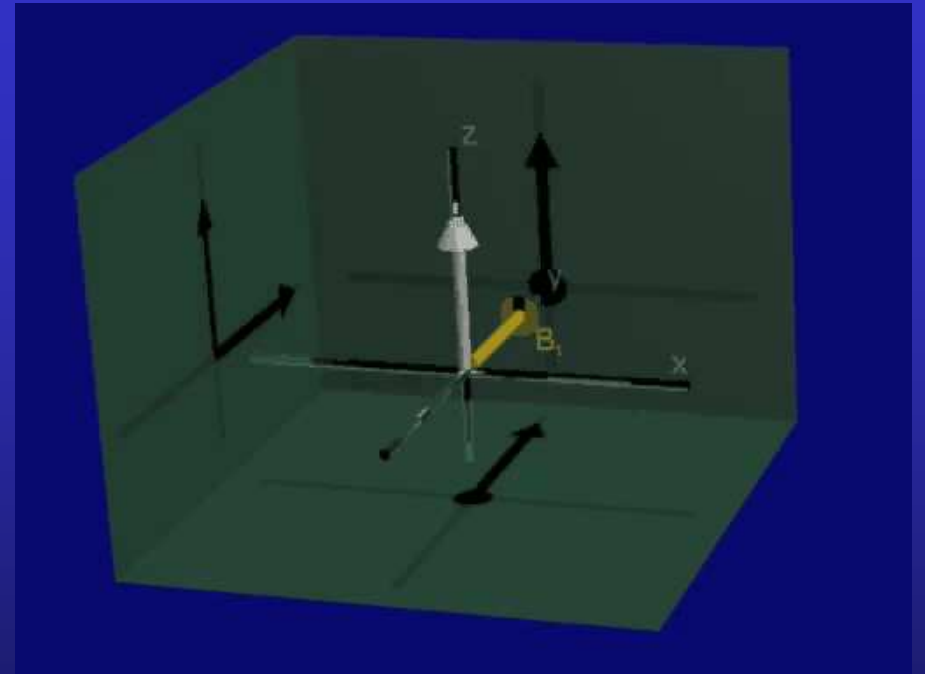
Receive Sensitivity

$$B_- = (B_x + jB_y)/2$$



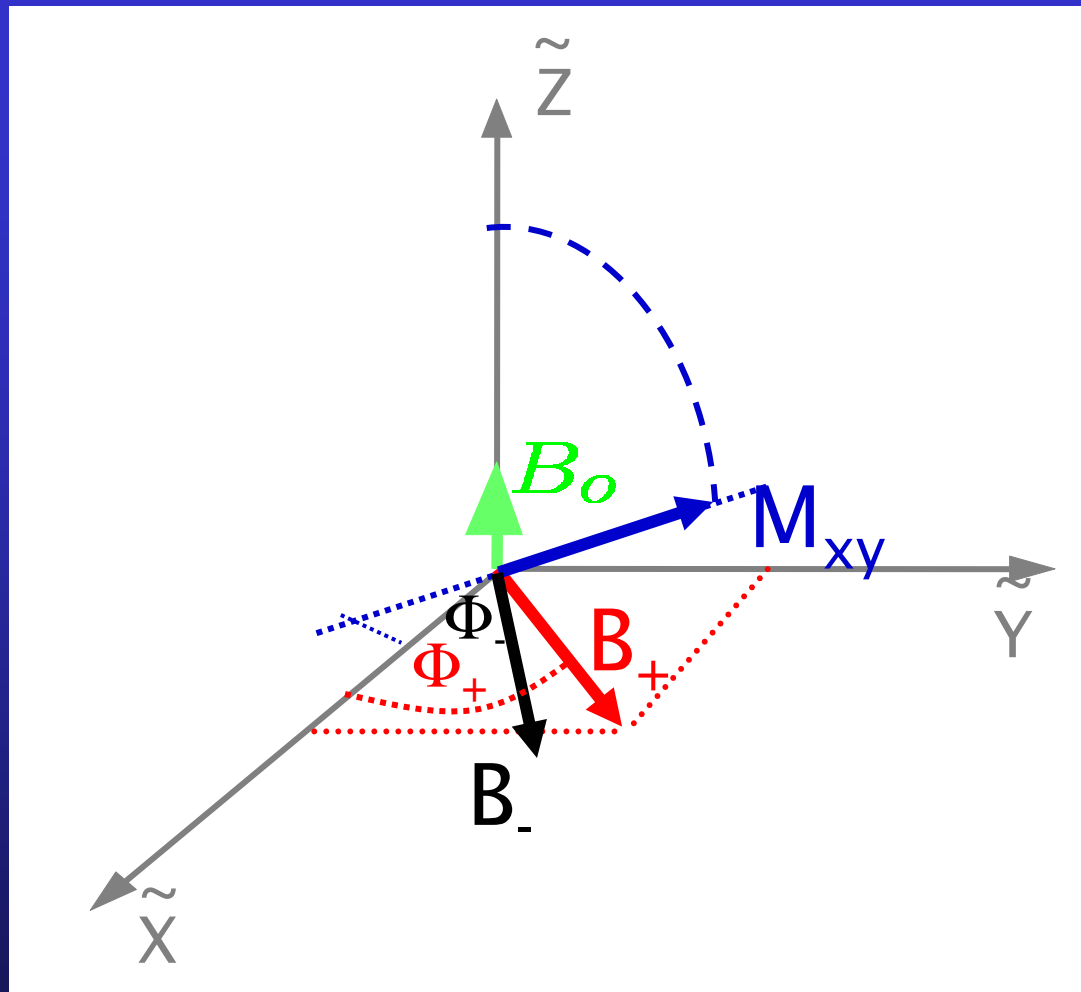
$$\vec{B}_L = (B_x - jB_y)(\hat{x} + j\hat{y})/2$$

$$\frac{d\vec{M}}{dt} = \gamma \vec{M} \times \vec{B}$$



$$\vec{B}_R = (B_x + jB_y)(\hat{x} - j\hat{y})/2$$

$$V(\omega) = \frac{j2\omega}{I} \int \vec{B}_R \cdot \vec{M} dv$$

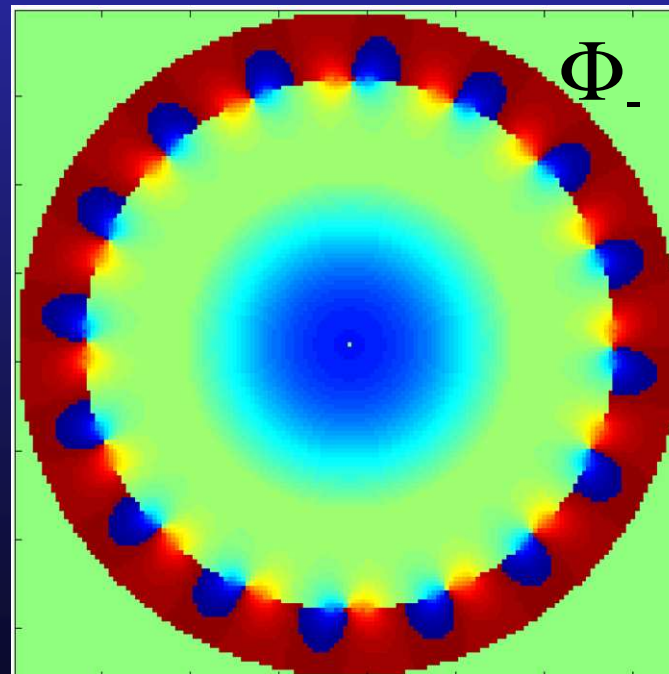
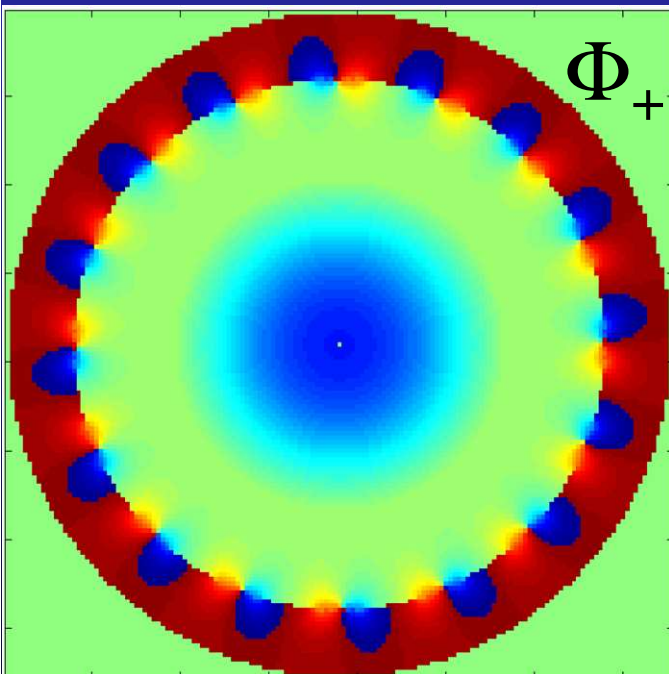
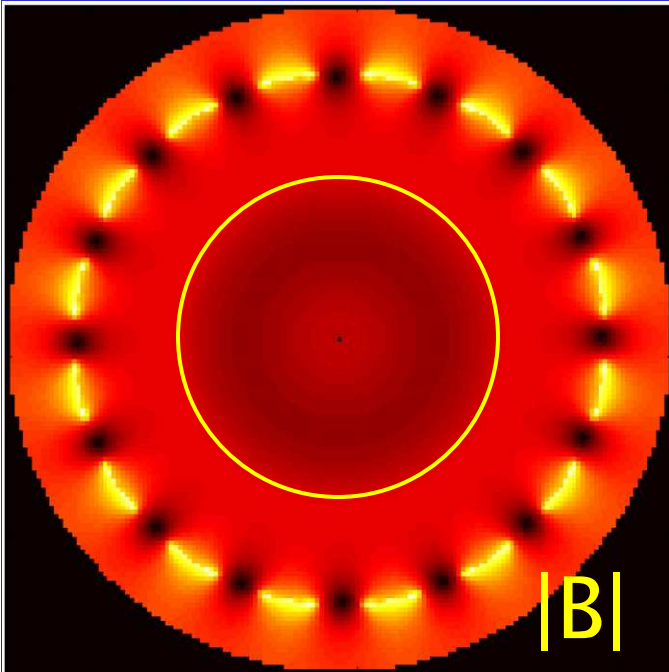


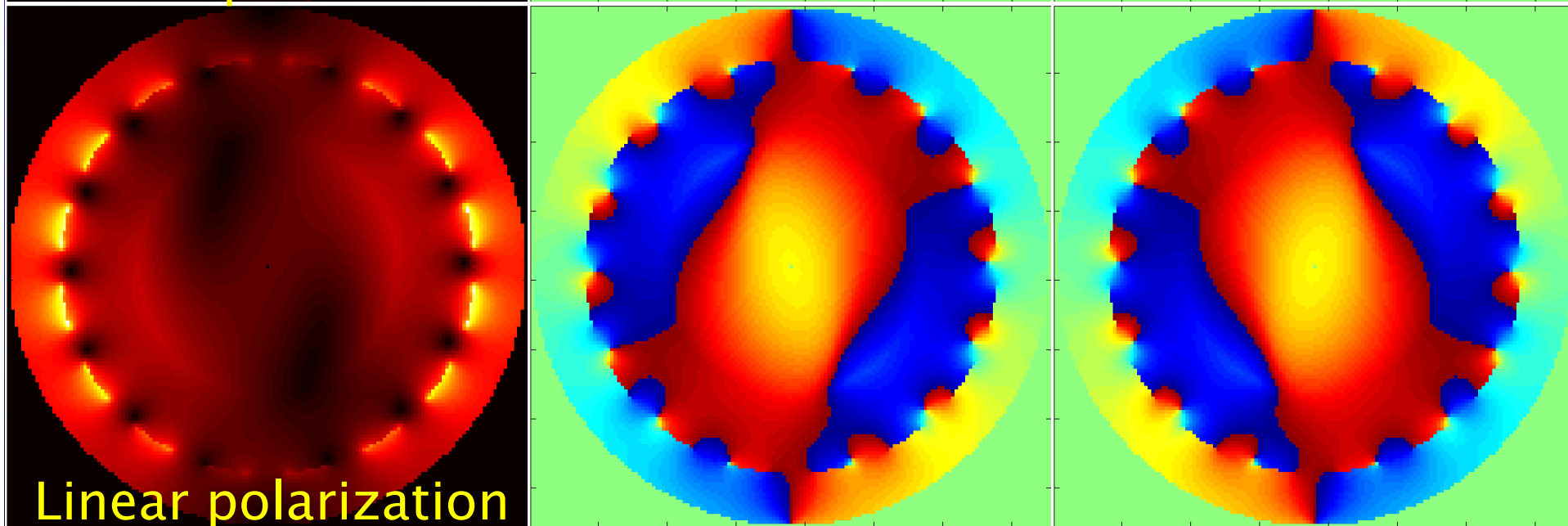
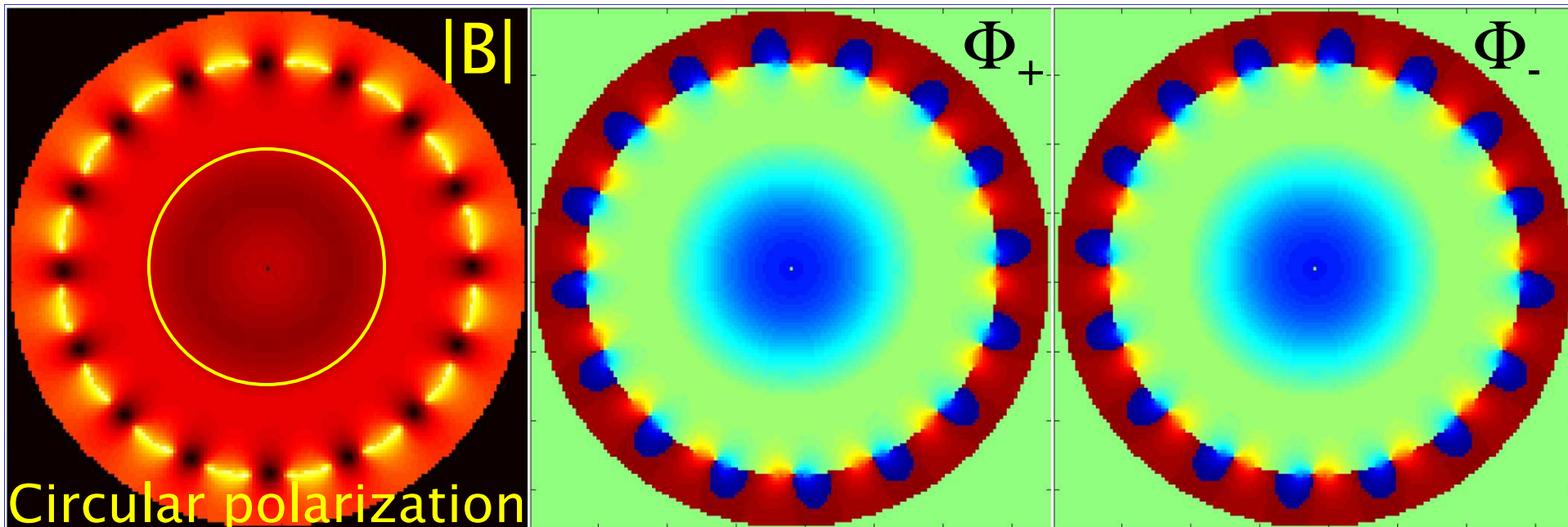
$$S = M_o \sin(c | B_+ |) | B_- | e^{j(\phi_+ + \phi_-)}$$

$\phi_- \approx \phi_+$ Is a good (needed) approximation.

Birdcage Tx,Rx Fields

64 cm birdcage, 80 cm shield, 40 cm sample.

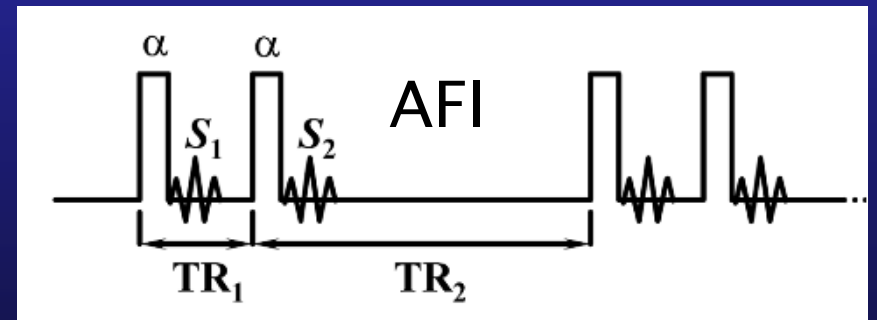
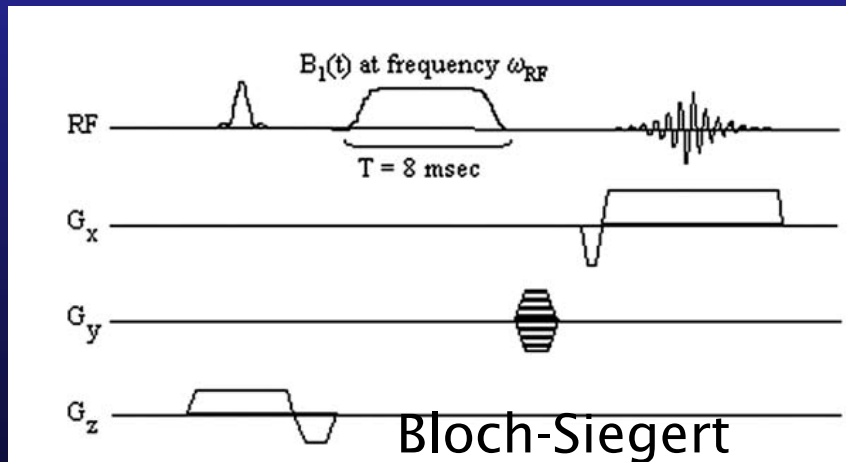




64 cm birdcage, 80 cm shield, 40 cm sample.

$|B_+|$ -Mapping

- Flip angle ratio (Double Angle) 90° limit, slow
- Actual Flip Angle, fast, 90° limit.
- Bloch Siegert – fast, phase based, but RF is 2nd order encoded.
- How to get high dynamic range?



Yarnykh et al., MRM 57:192, 2007.

Sacolick, MRM
63:1315, 2010

$$\omega_{BS} = \frac{(\gamma B_+)^2}{2\Delta\omega}$$

$$r \approx \frac{1 + \frac{TR_2}{TR_1} \cos \alpha}{\frac{TR_2}{TR_1} + \cos \alpha}$$

B1 Mapping Sequences

B1 Magnitude

- AFI (Yarnykh MRM 57,192,2007).
- MTM (Voigt MRM 64:725, 2010).
- Adiabatic (Shultz)
- Rotary echo (Scott)
- Phase-Sensitive Flip angle maps (Morrell)
- Bloch-Siegert(Sacolick).

B1 Phase

- Must refocus or calibrate out Bo.
- Spin Echo
- Fast Spin Echo
- Steady State Free Precession.
- Multi-TE GRE.

Electric Properties Tomography

Field Equations

$$\nabla^2 \vec{H} = j\omega\mu(\sigma + j\omega\varepsilon)\vec{H} \rightarrow \begin{aligned} \nabla^2 H_x &= j\omega\mu(\sigma + j\omega\varepsilon)H_x \\ \nabla^2 H_y &= j\omega\mu(\sigma + j\omega\varepsilon)H_y \end{aligned}$$

Transmit/Receive
Sensitivity Fields

$$H_+ = (H_x - jH_y)$$

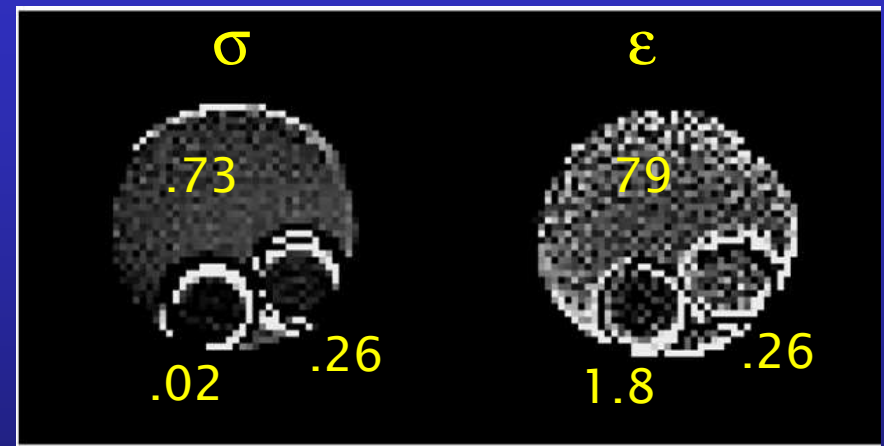
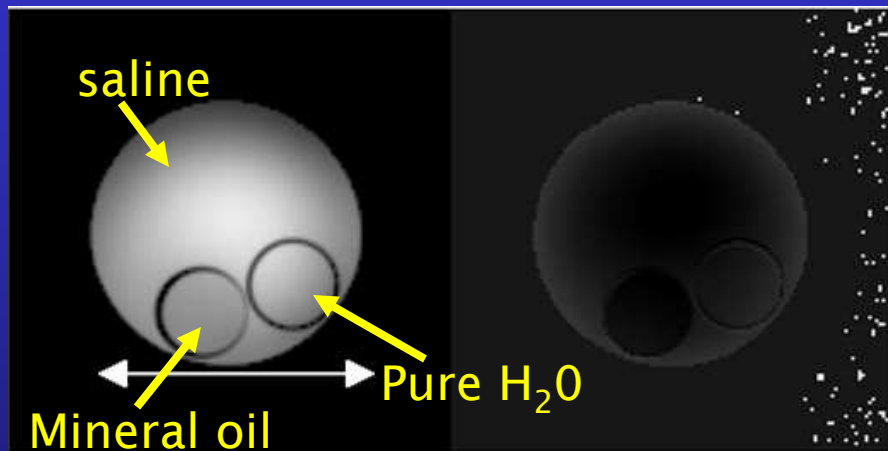
$$H_- = (H_x + jH_y)$$

$$\frac{\nabla^2 H_+}{H_+} = \frac{\nabla^2 H_-}{H_-} = j\omega\mu(\sigma + j\omega\varepsilon)$$

Non-invasive Quantitative Mapping of Conductivity and Dielectric Distributions Using the RF Wave Propagation Effects in High Field MRI

Han Wen Proc. SPIE 2003, 5030:471-477

National Heart, Lung and Blood Institute, National Institutes of Health, 10 Center Drive, Bethesda,



$$\sigma = \Im m \left[\frac{\nabla^2 H_+}{\omega \mu H_+} \right]$$

$$\epsilon = -\Re e \left[\frac{\nabla^2 H_+}{\omega^2 \mu H_+} \right]$$

$|B_+|$: Spin echo pair

$\Phi_+ \sim \Phi_i/2$ from spin echo phase

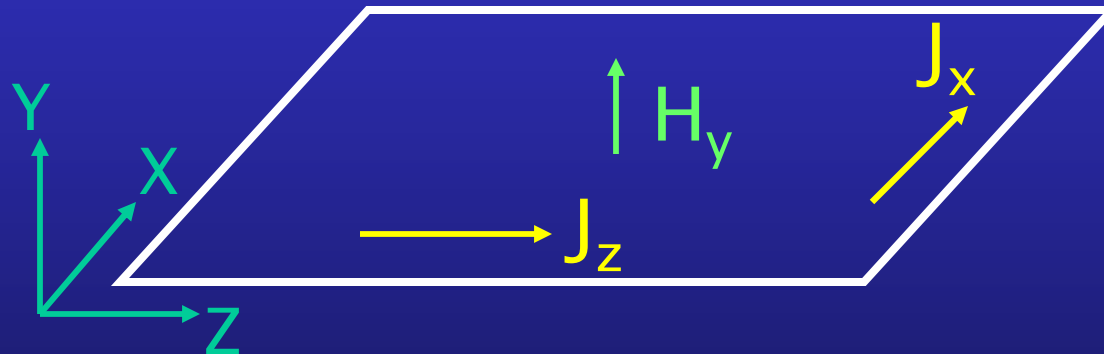
Bulumulla, 4467, ISMRM 2011, uses Bloch Segert $|B_+|$ & Spin echo Φ

Determination of Electric Conductivity and Local SAR Via B1 Mapping

U. Katscher, IEEE TMI 28, 1365, 2009

$$\nabla \times H = (\sigma + j\omega\epsilon)E = J \quad \int_A E \cdot dl = -j\omega\mu \int_A H \cdot da$$

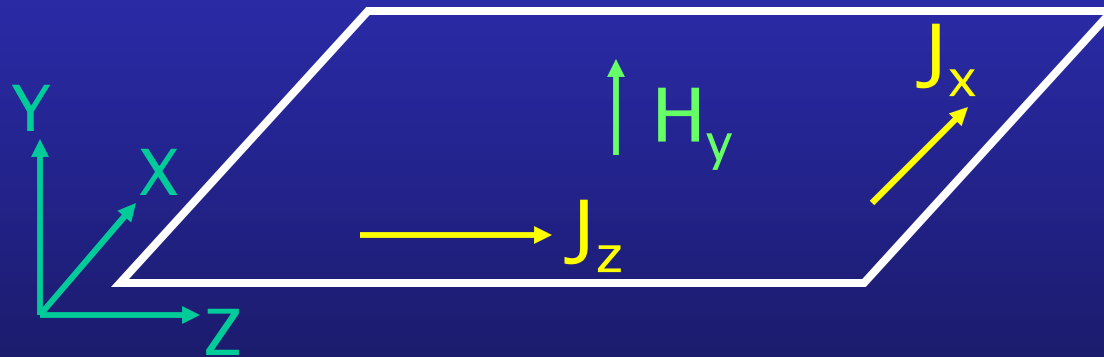
Ampere
Faraday



$$\frac{\oint_A \nabla \times H \cdot dl}{\omega^2 \mu \int_A H \cdot da} = \frac{\oint_A (\epsilon - j\sigma / \omega) E \cdot dl}{\int_A E \cdot dl} \approx \epsilon - \frac{j\sigma}{\omega}$$

Ampere's Law
Faradays's Law

$$\frac{\oint_A \left(\frac{\partial H_z}{\partial y} - \frac{\partial H_y}{\partial z} \right), \left(\frac{\partial H_y}{\partial x} - \frac{\partial H_x}{\partial y} \right) \cdot dl}{\omega^2 \mu \int_A H_y \cdot dx dz} \approx \epsilon - \frac{j\sigma}{\omega}$$



- In birdcage, TEM coil, $H_z \sim 0$.
- Tx/Rx phase: $\Phi = \Phi_+ + \Phi_- \sim 2\Phi_+$
- $B_+ = (B_x - jB_y)/2$ $B_- = (B_x + jB_y)/2$

Helmholtz Algorithm

$$-\oint_A \nabla H_+ \cdot da = \nabla^2 H_+ dV$$

$$\frac{-\oint_A \nabla H_+ \cdot da}{\omega^2 \mu \int_A H_+ dV} = \epsilon - \frac{j\sigma}{\omega}$$

$$-\frac{\nabla^2 H_+}{\omega^2 \mu H_+} = \epsilon - j \frac{\sigma}{\omega}$$

Voigt/Katscher EPT \longrightarrow \int Helmholtz equation

σ, ϵ constant in region, H_z unrestricted.

Magnitude & Phase

$$\nabla^2 H_+ = j\omega\mu(\sigma + j\omega\varepsilon)H_+ \quad H_+ = h_+ e^{j\phi_+}$$

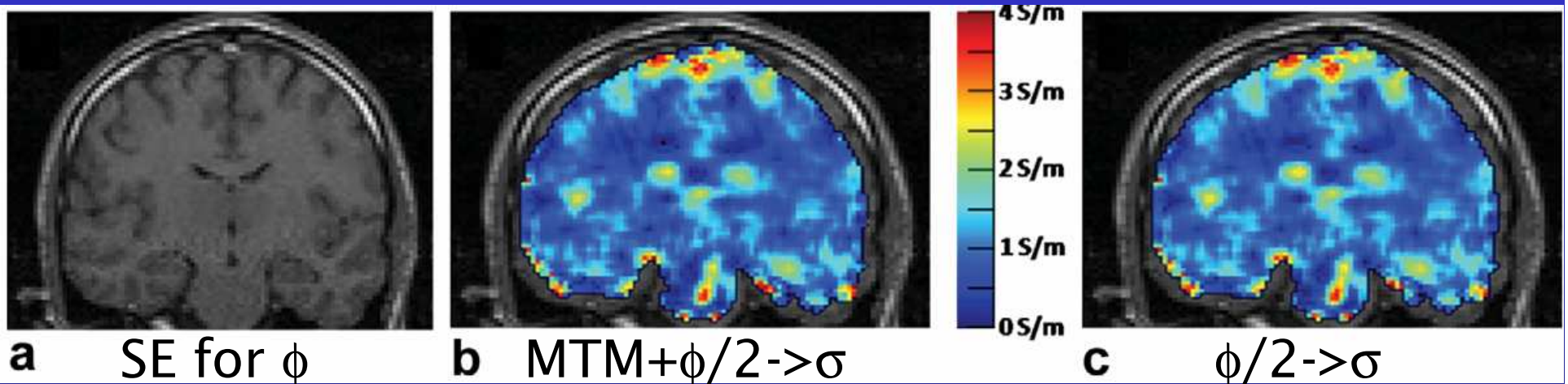
$$2\nabla\phi_+ \bullet \nabla \ln h_+ + \nabla^2 \phi_+ = \omega\mu\sigma$$

$$\frac{\nabla^2 h_+}{h_+} - |\nabla\phi_+|^2 = -\omega^2 \mu\varepsilon$$

Voigt, MRM 2011 epub,
19th ISMRM, 127, 2011

van Lier, 19th ISMRM,
125,4464, 2011

Quantitative Conductivity & Permittivity Imaging of the Human Brain Using Electric Properties Tomography, T. Voigt, U Katscher, O Doessel, MRM, epub 2011.



Phase based conductivity: +5 to 15% error vs “exact”

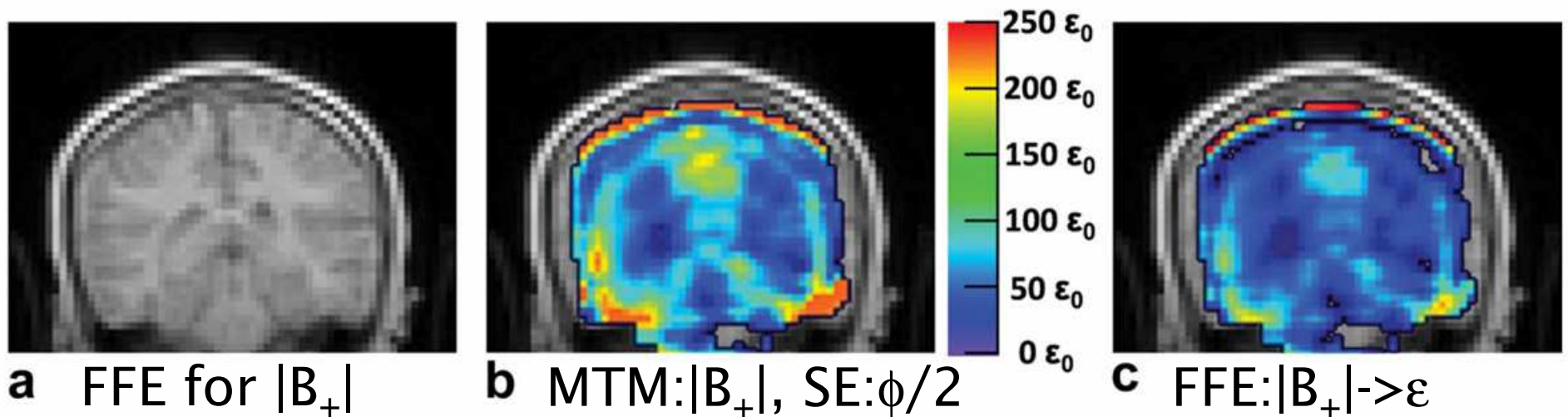


Image magnitude permittivity: -10 to 20% error vs “exact”

Glioma Tissue Conductivity T.

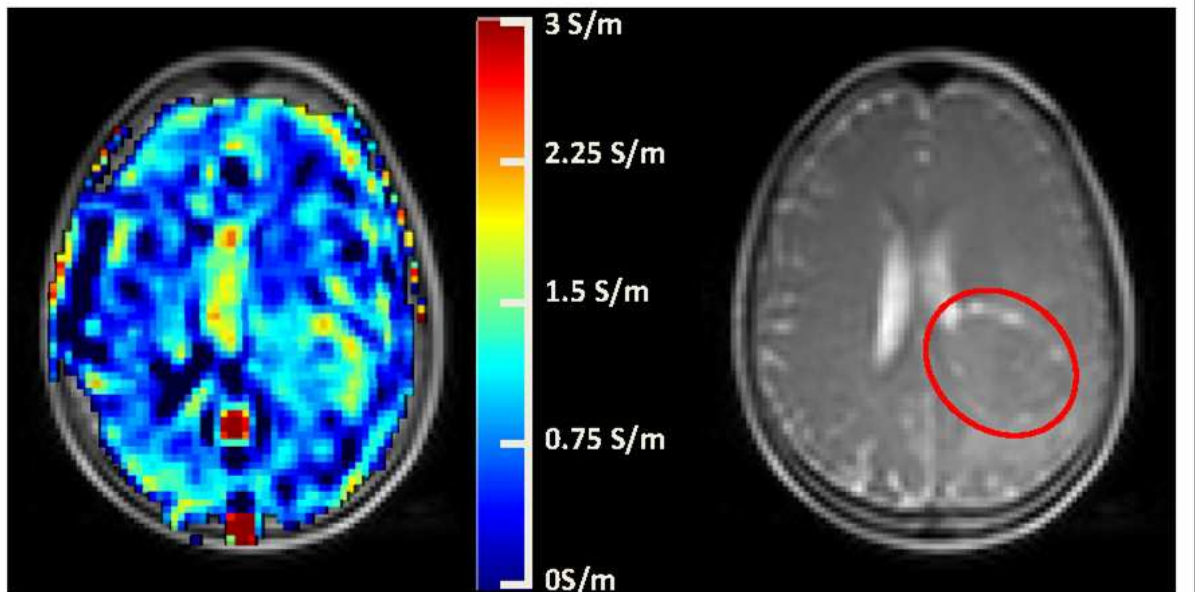
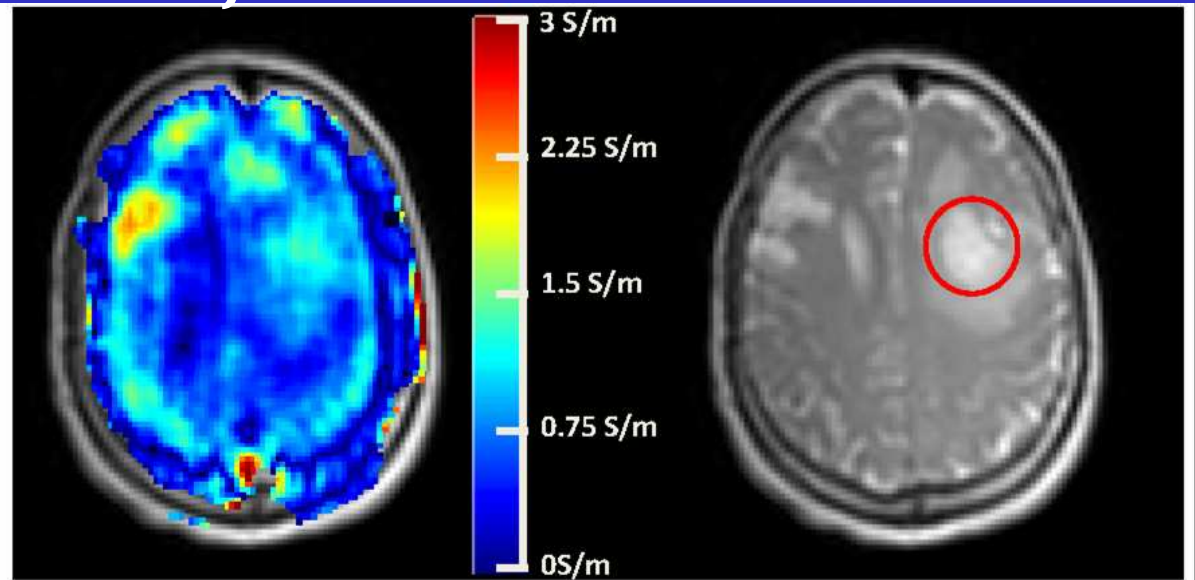
T. Voigt, 127, ISMRM 2011

pat.	white matter	glioma
1	0.36 ± 0.12	0.97 ± 0.18
2	0.38 ± 0.22	1.02 ± 0.37

Phase based σ map

3D FSE

$$\frac{\nabla^2 \phi_+}{\omega \mu} = \sigma$$



Real-Time Conductivity Mapping using Balanced SSFP and Phase-Based Reconstruction, C Stehning, 128, ISMRM 2011

Use SSFP to acquire phase, and conductivity with salt-water phantom.

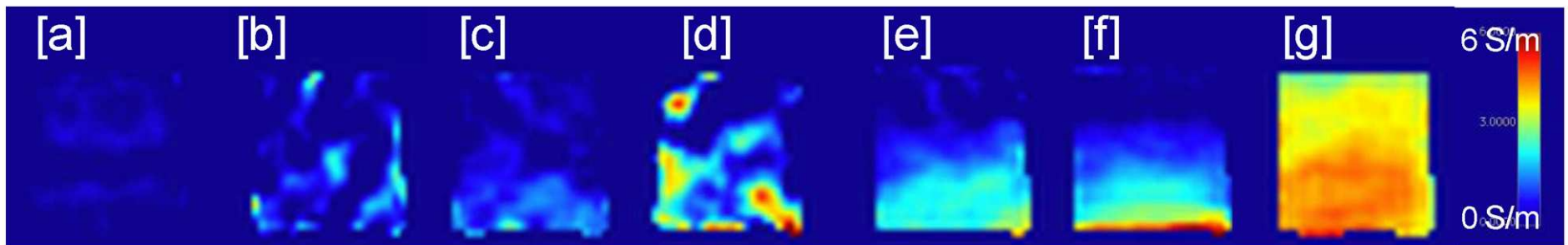
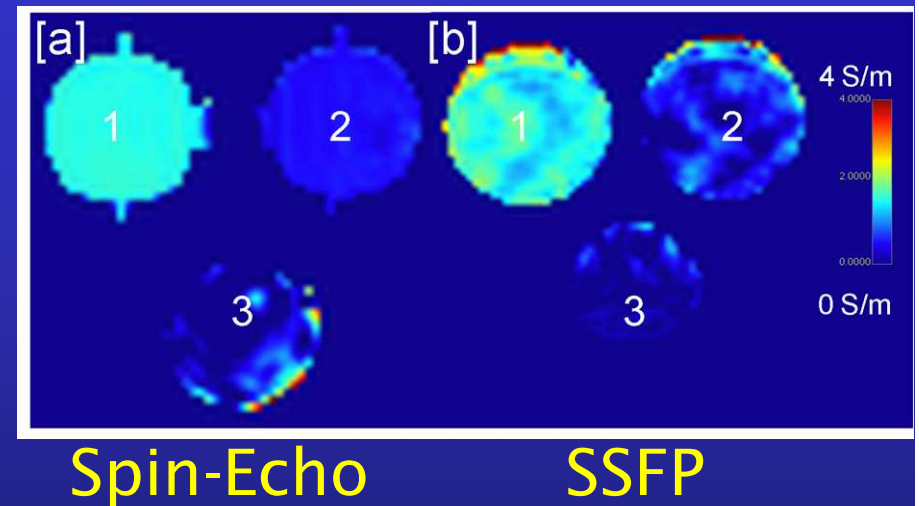


Fig. 3 Series of SSFP real-time conductivity maps in tab water. [a] initial condition, [b, c, d] during addition of salt, [e, f] at three minutes intervals, [g] after stirring.

Comparing EPT at 1.5, 3 & 7T, A. van Lier, p125, ISMRM 2011

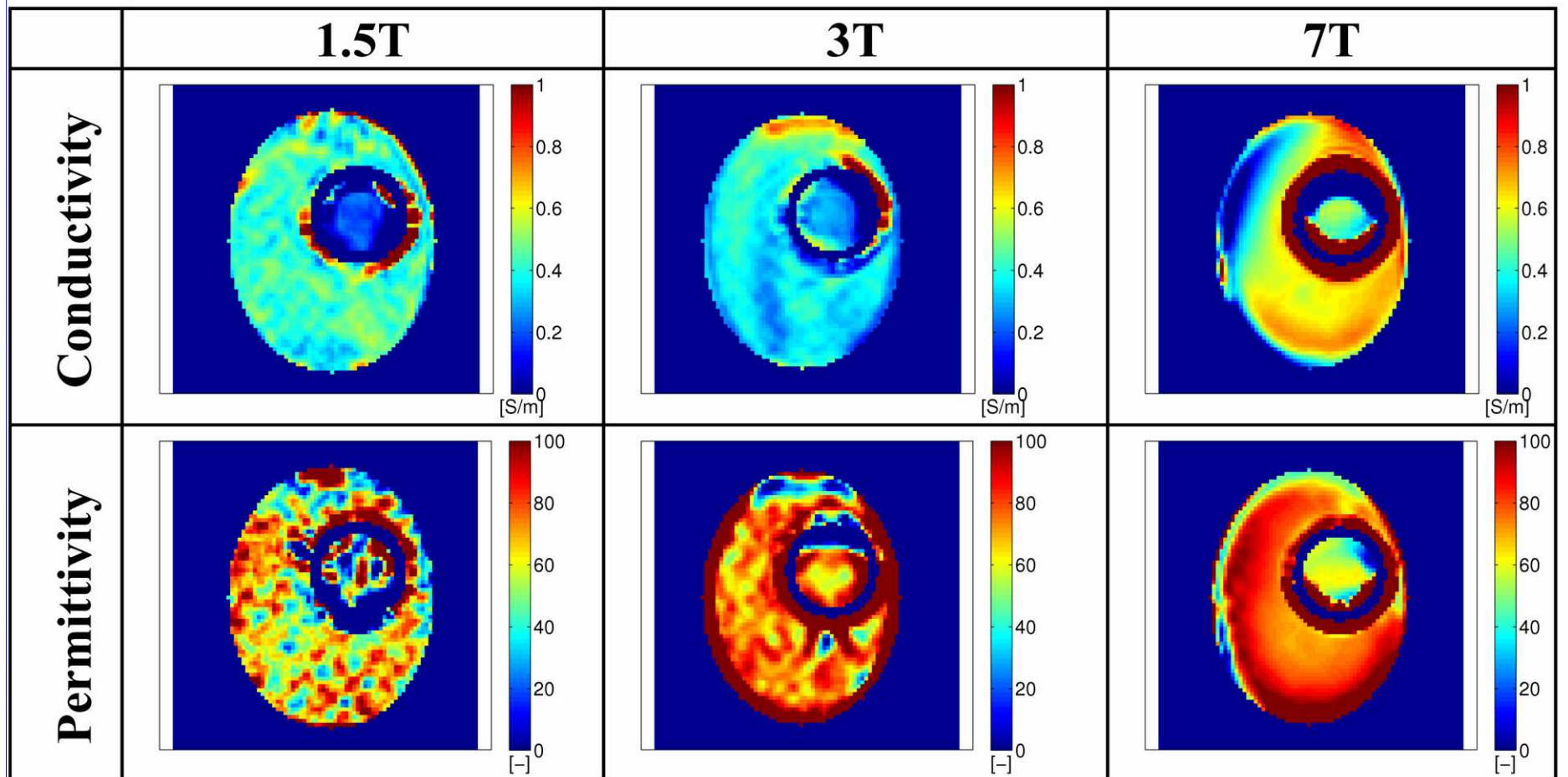


Figure 2: Reconstructions based on measurements of $|B_1^+|$ and φ_m at different field strengths.

B1 phase: Spin echo, $|B_+|$: AFI (3&7T), DAM (1.5T)

Electrical Conductivity Imaging of Brain Tumours, A. van Lier, 4464, ISMRM 2011

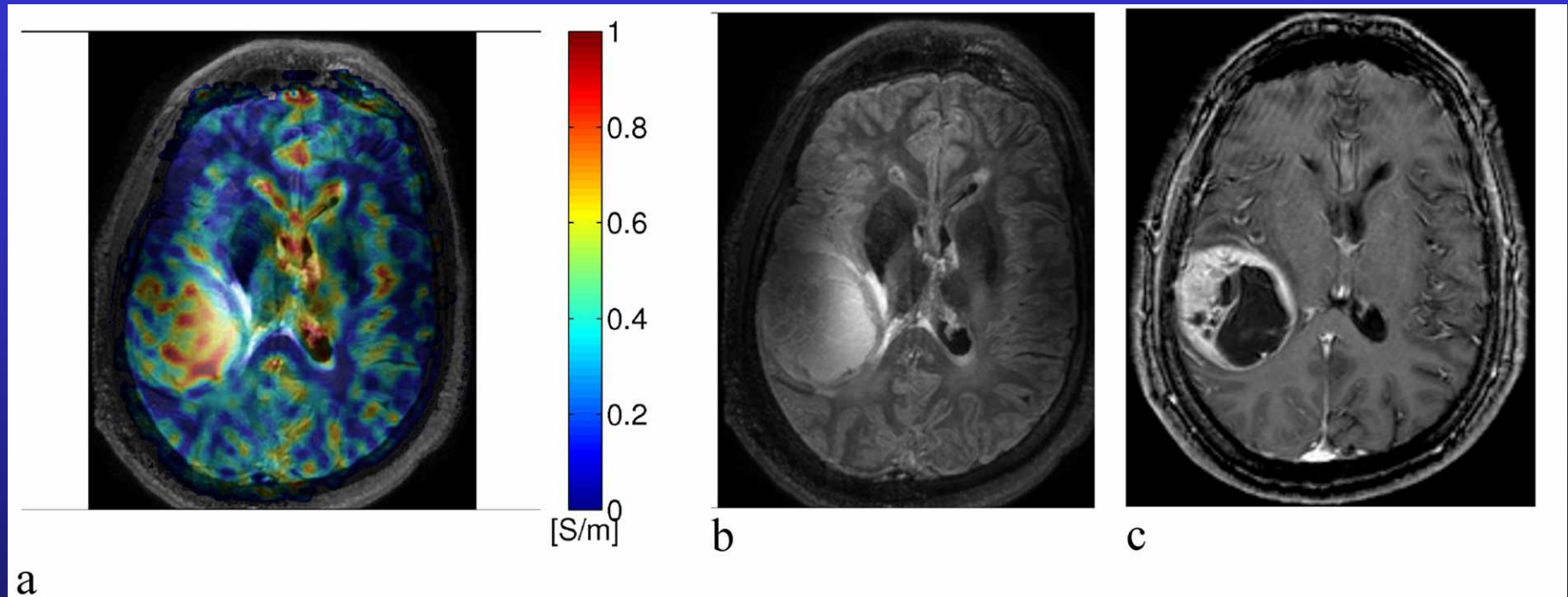


Figure 2: Patient 1: grade IV astrocytoma a) Reconstructed conductivity map overlaid on a FLAIR image. b) FLAIR c) post-contrast 3T T1W

$$2\nabla \phi_+ \cdot \nabla \ln h_+ + \nabla^2 \phi_+ = \omega \mu \sigma$$

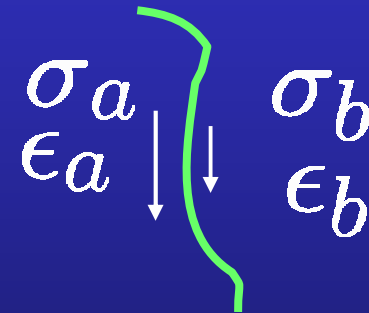
|B+|: Bloch-Siegert, Phase: Two interleaved GRE

RF Current Density Imaging

Current Density Contrast

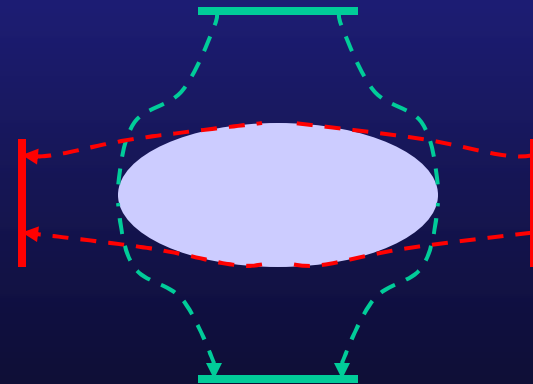
Tangential current ratio equals ratio of complex conductivity. Normal current yields no contrast.

$$\frac{J_{at}}{J_{bt}} = \frac{(\sigma + j\omega\epsilon)_a}{(\sigma + j\omega\epsilon)_b}$$



~2 orthogonal injections to visualize tangent.

$$\nabla^2 \mathbf{H} = \mathbf{J} \times \frac{\nabla \sigma^*}{\sigma^*}$$



Quasi-Static Field Equations

$$\nabla^2 \vec{H} = j\omega\mu(\sigma + j\omega\epsilon)\vec{H} + \vec{J} \times \frac{\nabla(\sigma + j\omega\epsilon)}{(\sigma + j\omega\epsilon)}$$

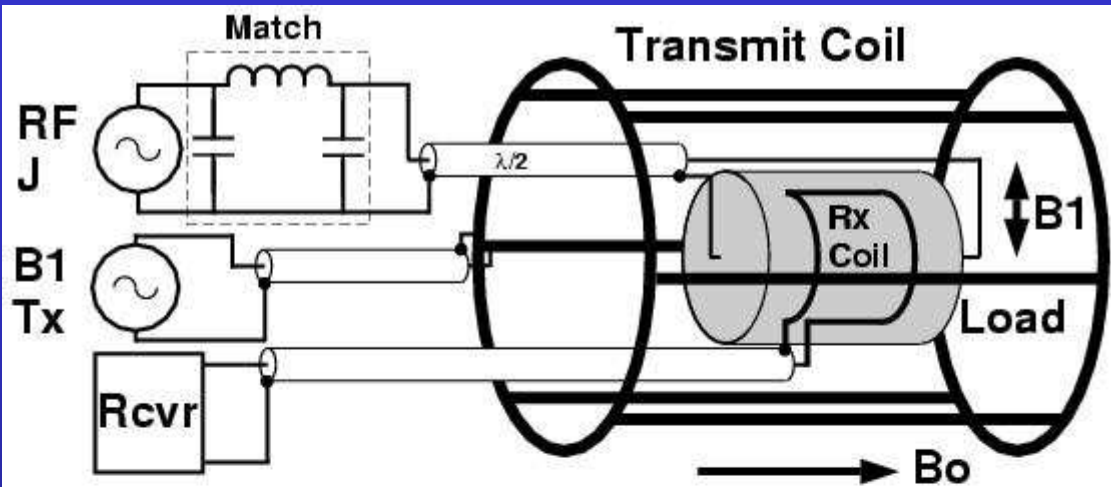
Wave eqn


$$\nabla^2 \vec{H} = \nabla(\sigma + j\omega\epsilon) \times \nabla V$$

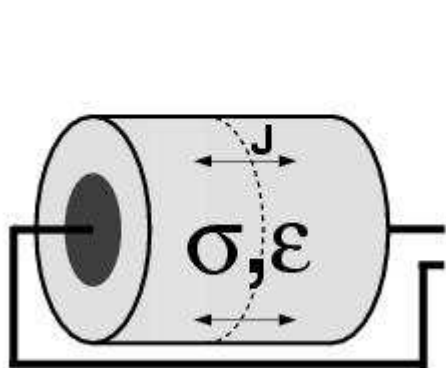
Poisson/Laplace

$$\nabla \times \vec{H} = \vec{J}$$

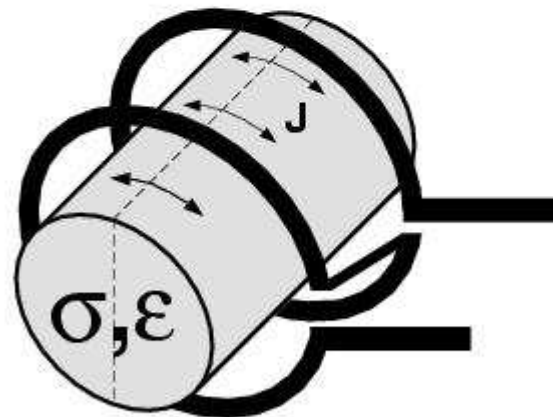
Two Channel Parallel Transmit : Birdcage + Electrode



a) Physical Layout



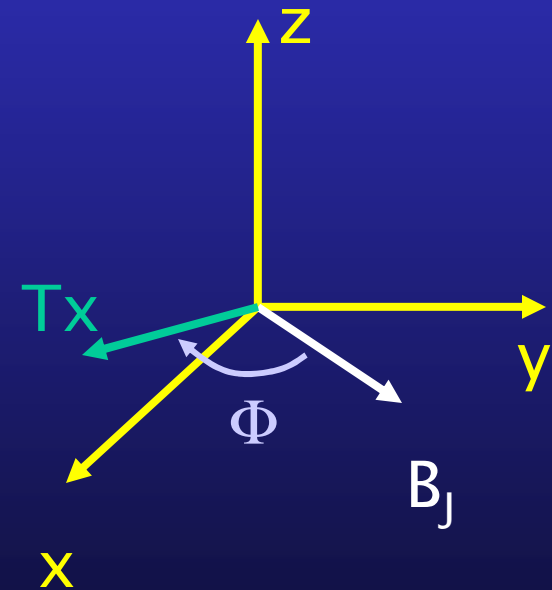
**b) Capacitive/
Resistive
Coupling**



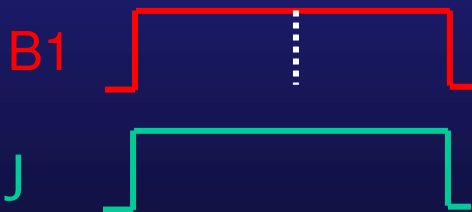
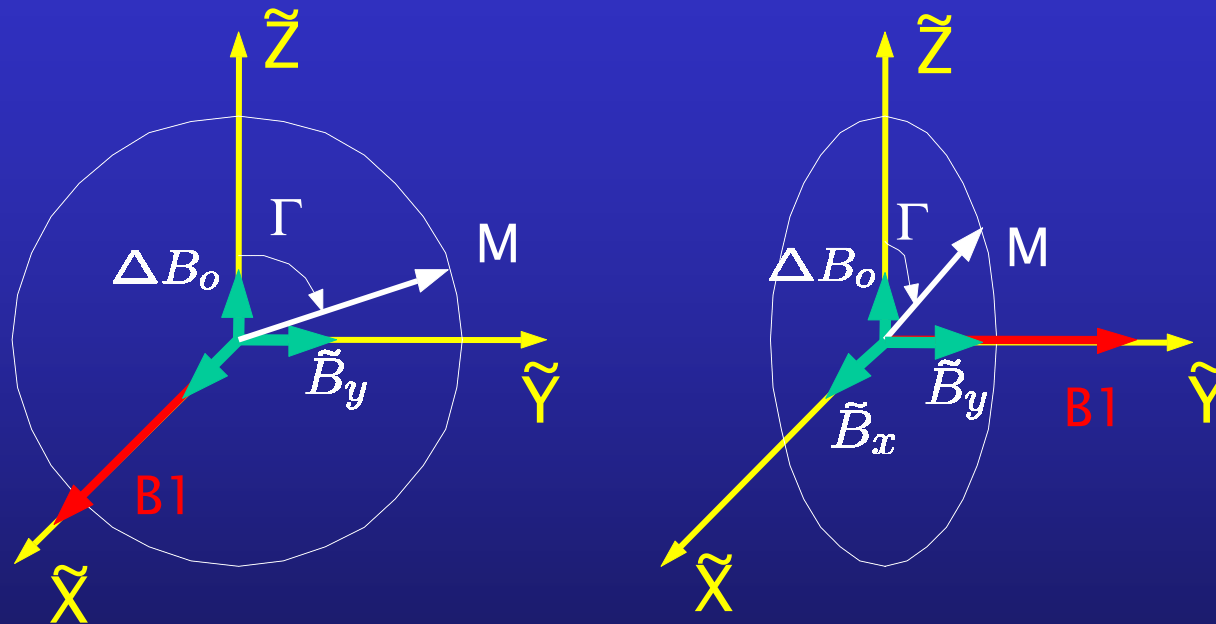
**c) Inductive
Coupling**

Birdcage is transmit phase reference.

Rcv phase cancelled.



Rotating Frame Prep

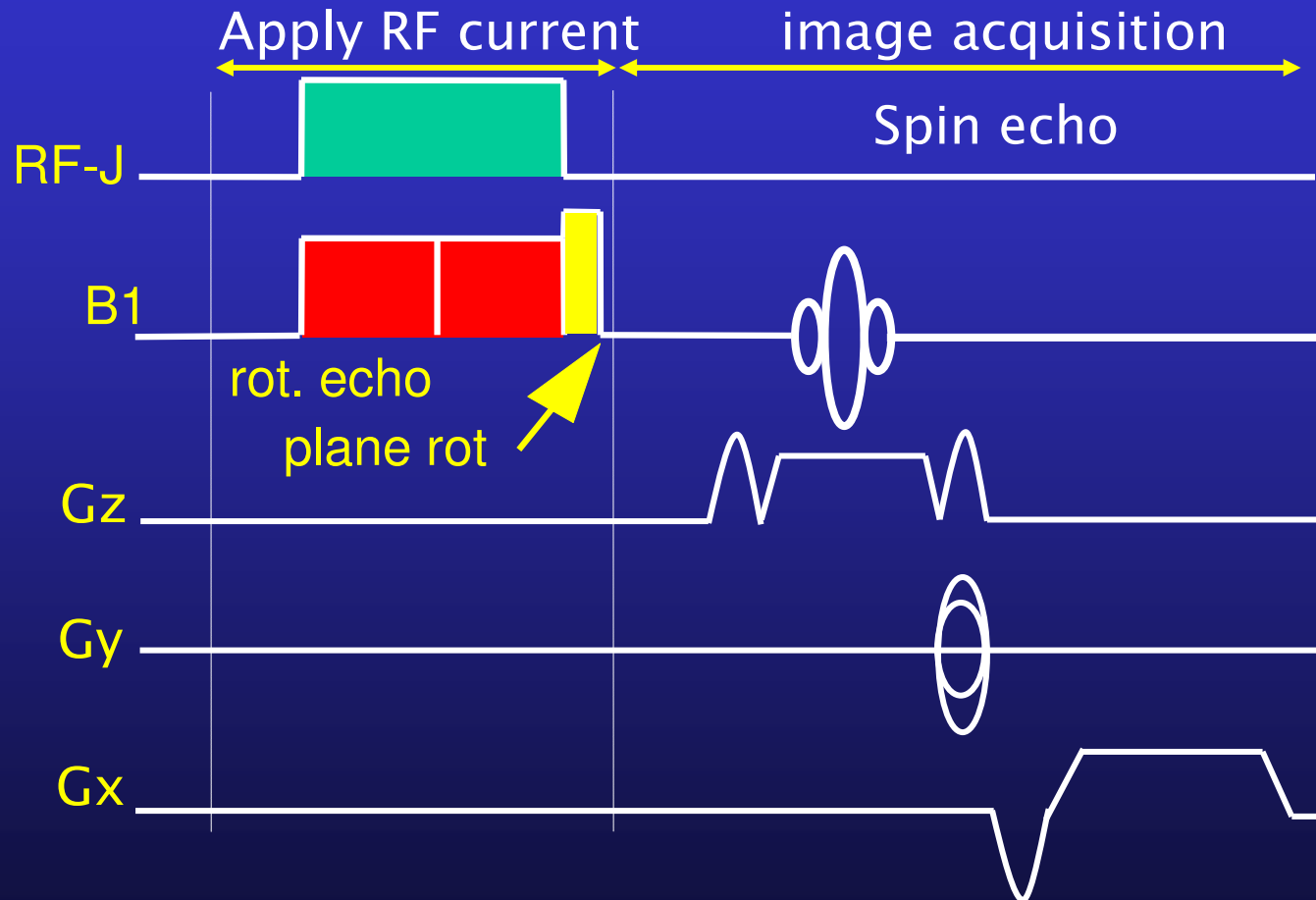


$$\Gamma_x = -\gamma T_c (\tilde{B}_x + B_1)$$

$$\Gamma_x = -\gamma T_c \tilde{B}_x \quad (\text{Rotary echo})$$

MRI can map RF magnetic fields created by the ablation current.

Rotary Echo Imaging Sequence



Acquire 4 interleaved sets. Construct phase map images.

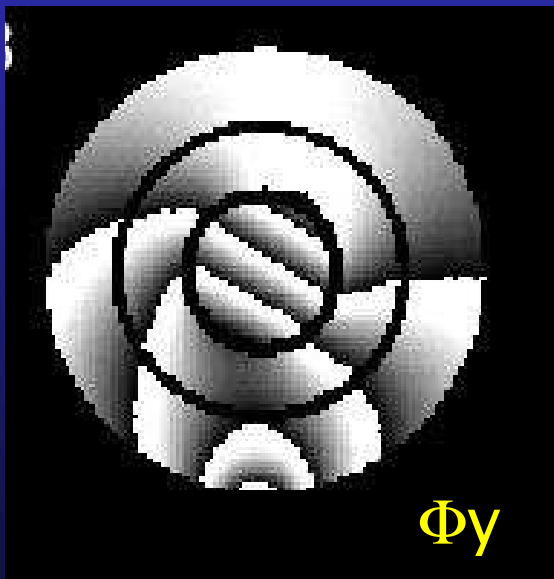
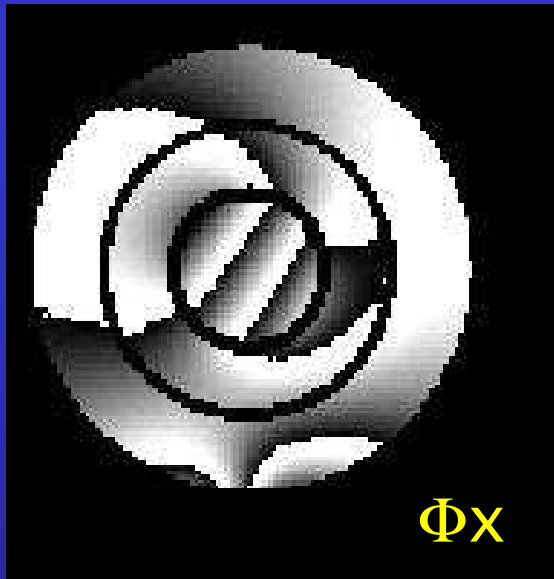
Rotating Frame Current

If the rotating frame fields are measured, we compute

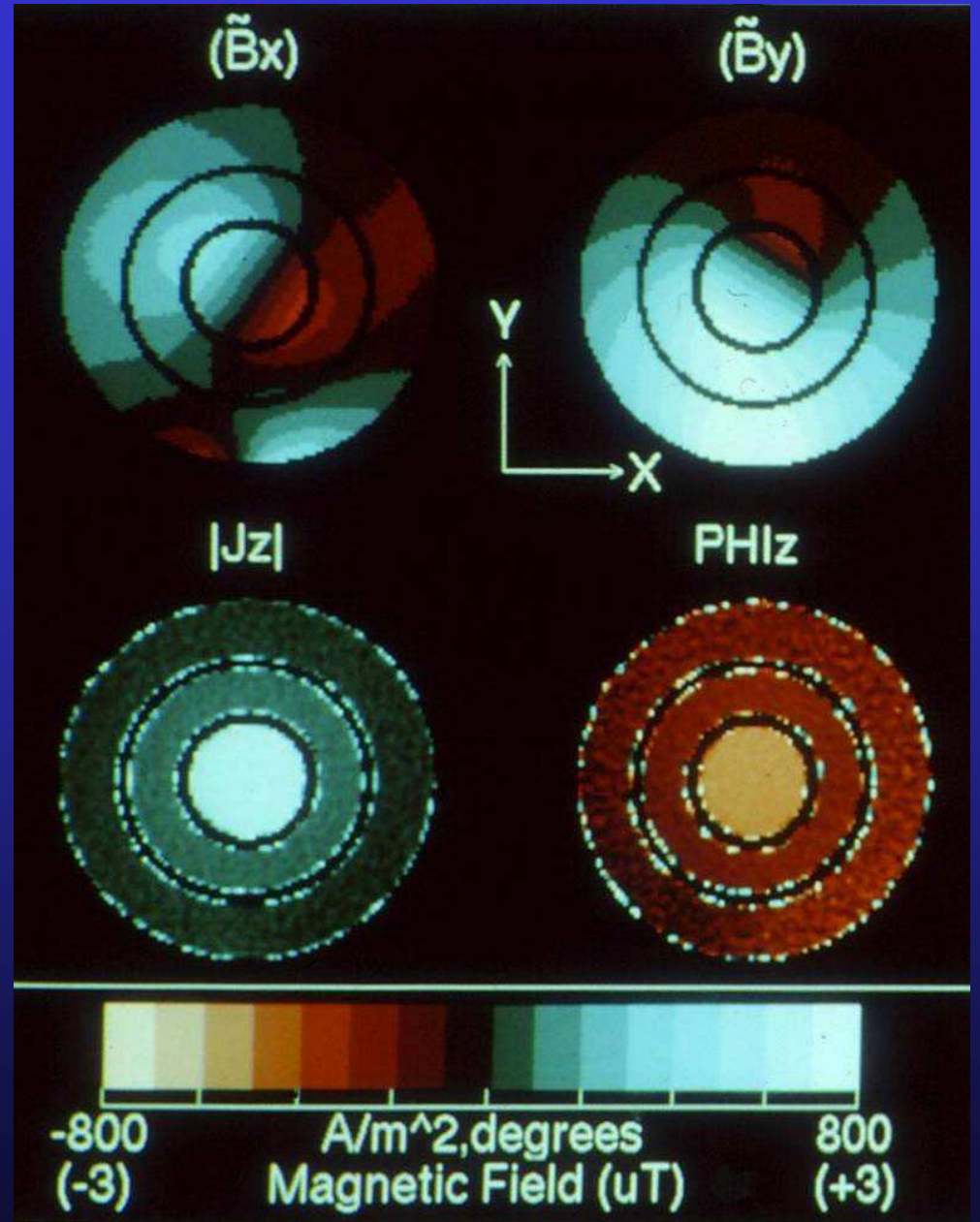
$$\tilde{J}_z = |\tilde{J}_z| e^{j\phi} = 2 \left[\frac{\partial \tilde{H}_y}{\partial x} - \frac{\partial \tilde{H}_x}{\partial y} \right] + 2j \left[\frac{\partial \tilde{H}_x}{\partial x} + \frac{\partial \tilde{H}_y}{\partial y} \right]$$

Result mixes true J_z and an error term we can control.

$$\tilde{J}_z(\phi) = \underbrace{j_z \cos(\phi_z - \phi - \psi)}_{\text{Correct current}} + \underbrace{\partial / \partial z [h_z \sin(\theta_z - \phi - \psi)]}_{\text{Error term}}$$



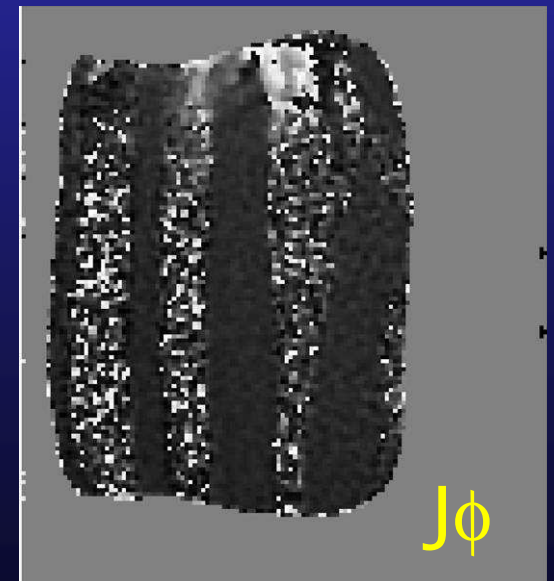
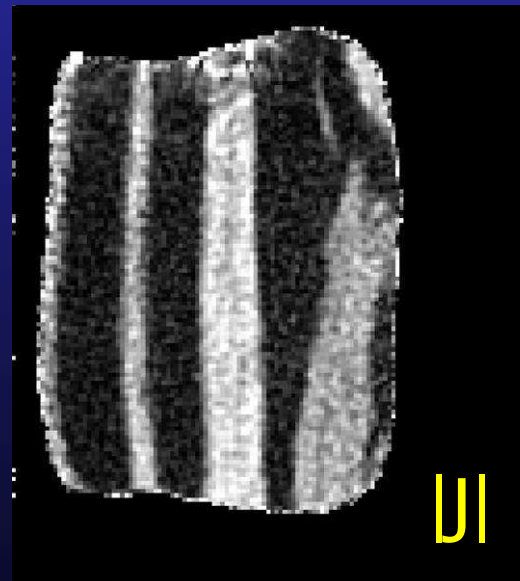
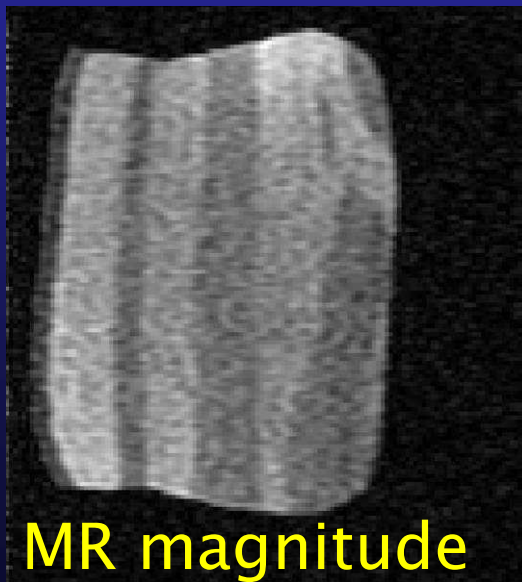
Raw B1 phase maps



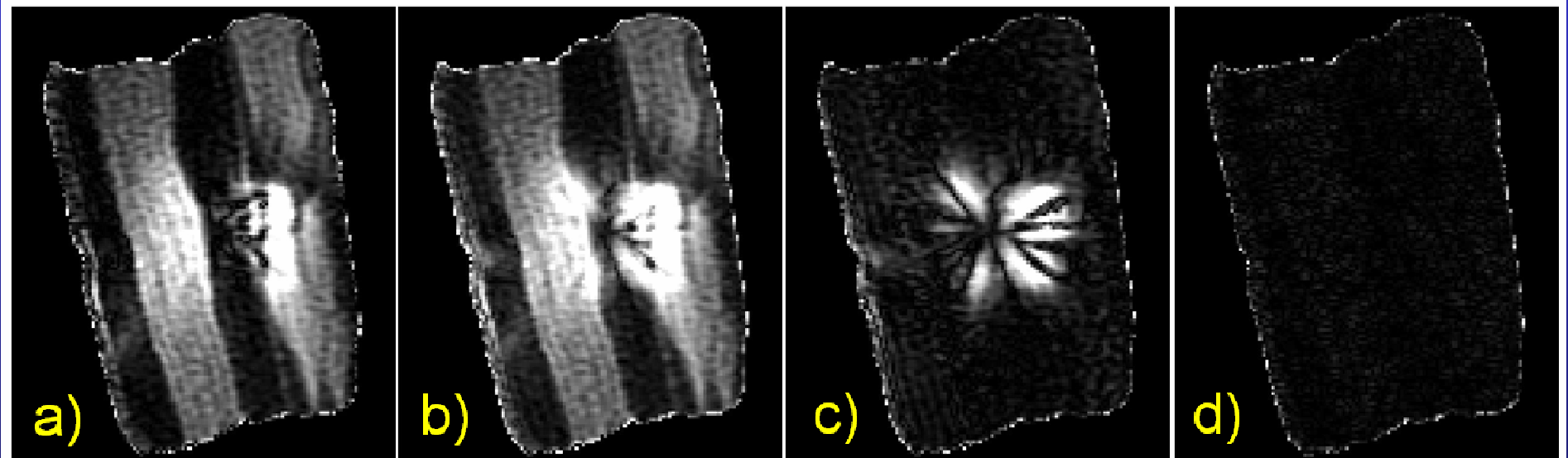
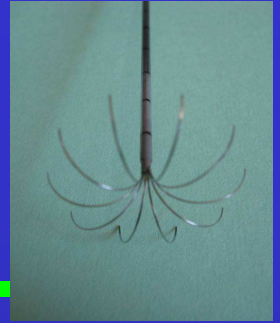
Pork Sample: 21.3 MHz



256x256 (cropped)
FOV 16cm, slice
5mm TR:300ms, TE
16ms



Equi-phase Condition



$|z|, \Phi$ constant

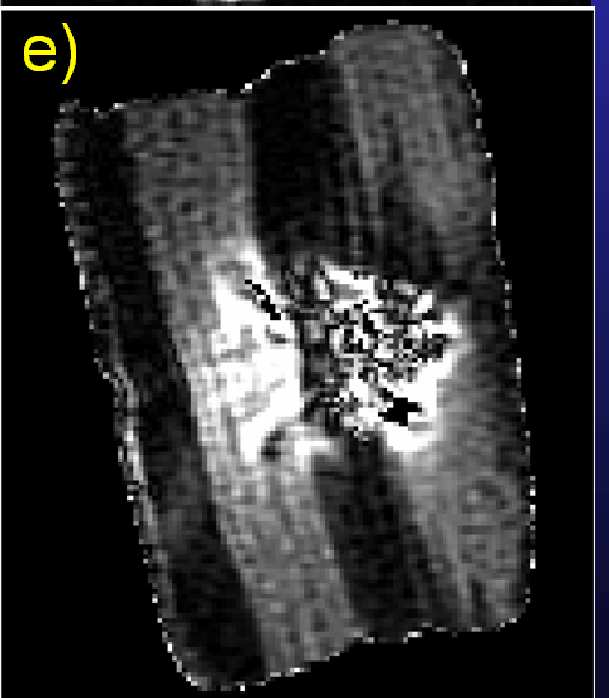
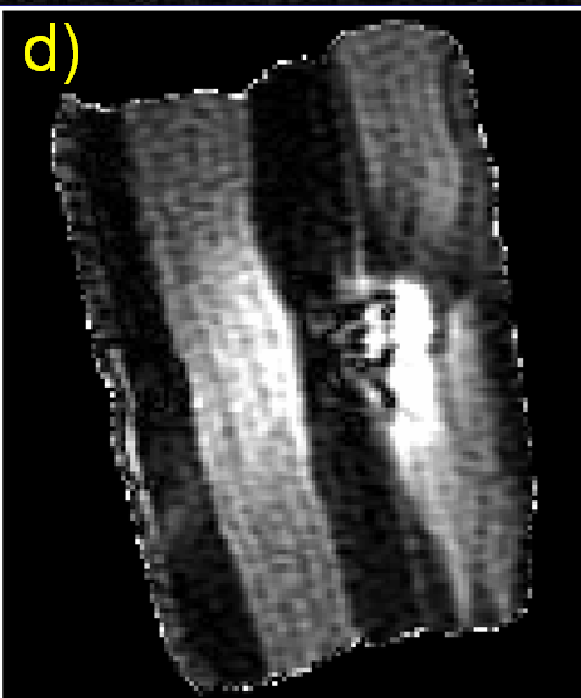
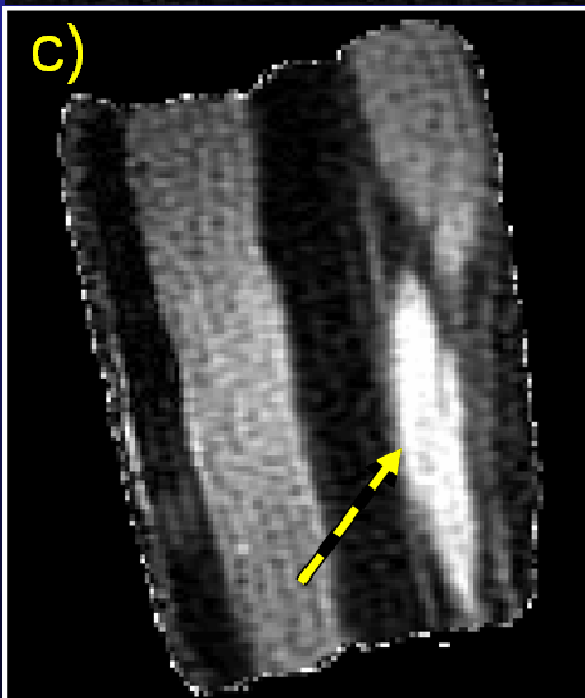
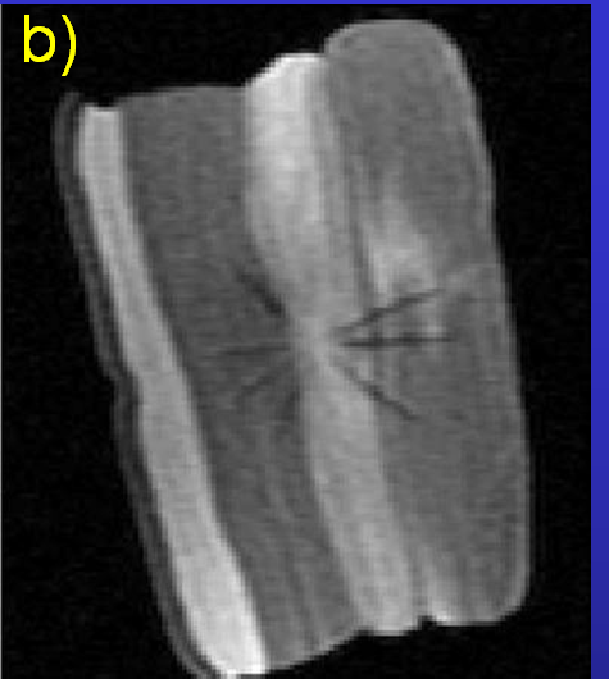
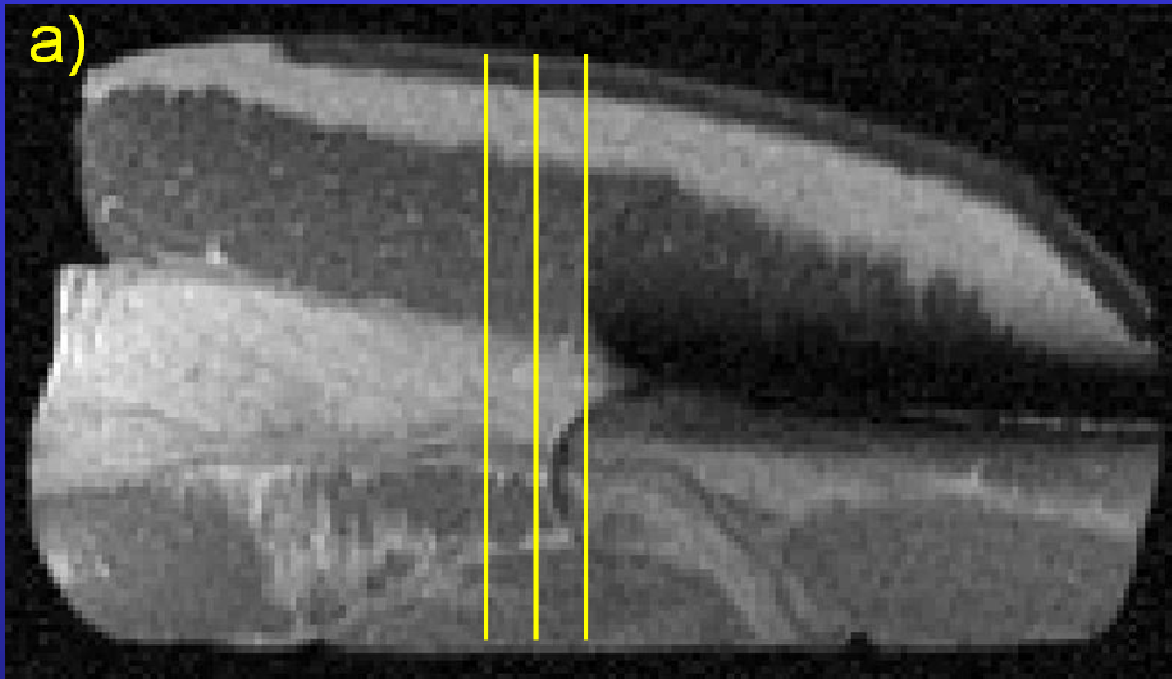
$|z|, \Phi$ free

dHz/dz

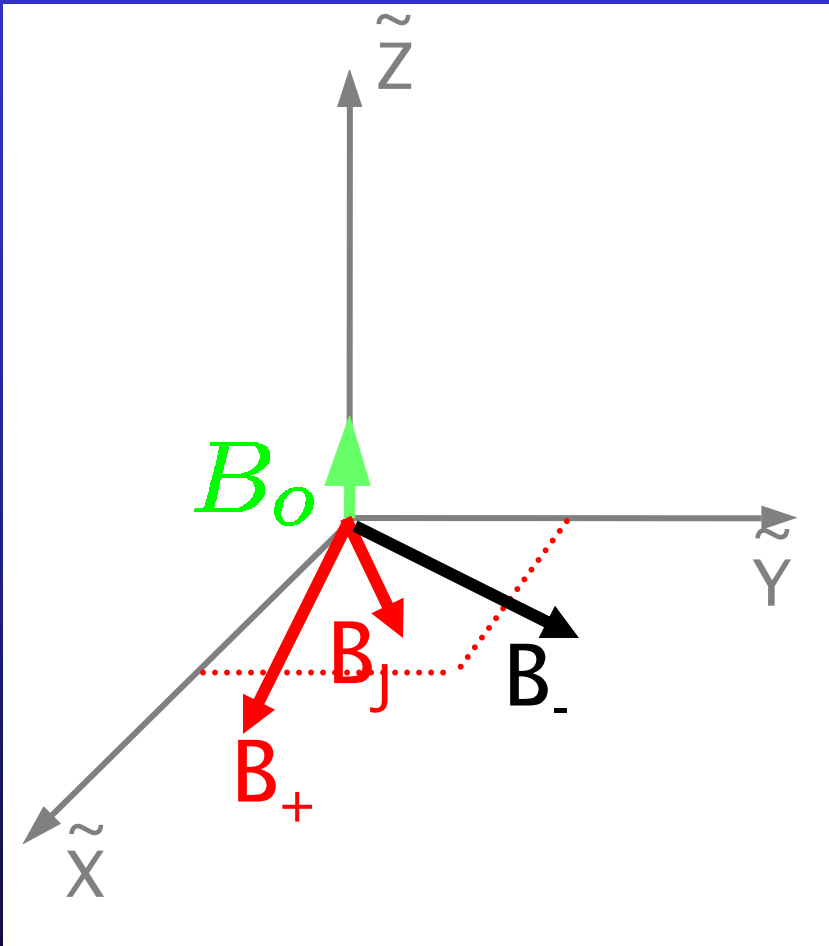
No current

$$\vec{B}_+ = (|B_x| - j|B_y|)e^{j\phi}(\hat{x} + j\hat{y})/2$$

For linearly polarized fields, a single global phase correction can be found, and dHz/dz artifacts eliminated.



RF Current Imaging



RF J phase = $\Phi_j - \Phi_+$

Electric Properties

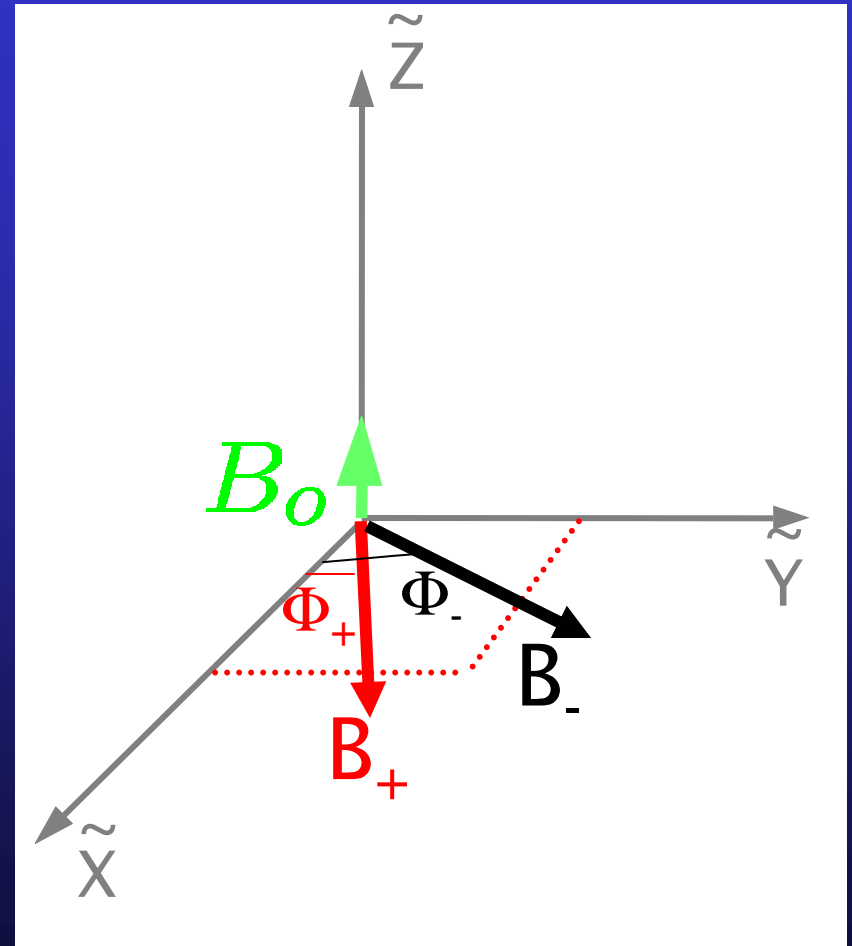
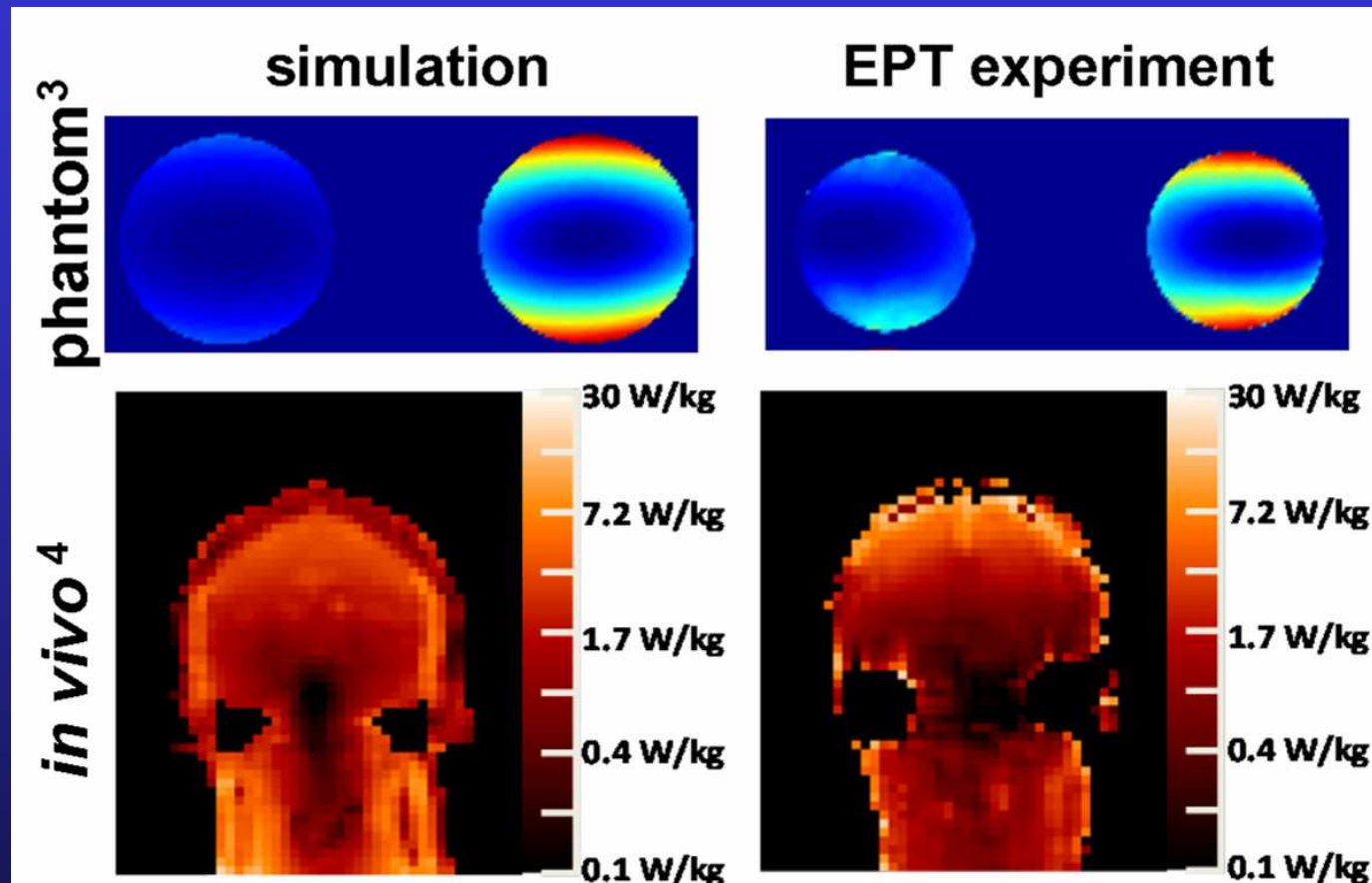


Image Phase = $\Phi_+ + \Phi_-$

New Directions

Single Element SAR Measurements in a Multi-Transmit System, U. Katscher, 494, ISMRM 2011



$$SAR = \sigma |E|^2 = |\nabla \times H|^2 / \sigma \quad H_z \approx 0$$

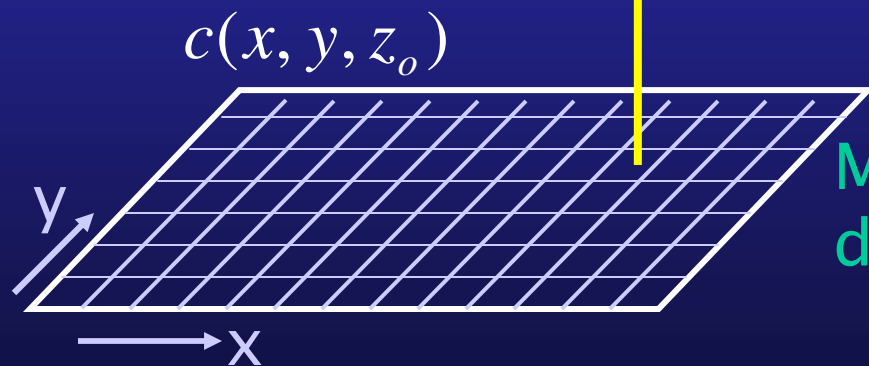
EPT+RFCDI

Also, U. Katscher, MRII, Seoul 2010

Recovering Hz: $\nabla \cdot \vec{H} = 0$.

$$\nabla \cdot \vec{H} = 0 \rightarrow \frac{\partial H_z}{\partial z} = -\left(\frac{\partial H_x}{\partial x} + \frac{\partial H_y}{\partial y}\right)$$

$$H_z(x, y, z) = -\int_{z_0}^z \left(\frac{\partial H_x}{\partial x} + \frac{\partial H_y}{\partial y}\right) dz + c(x, y, z_0)$$



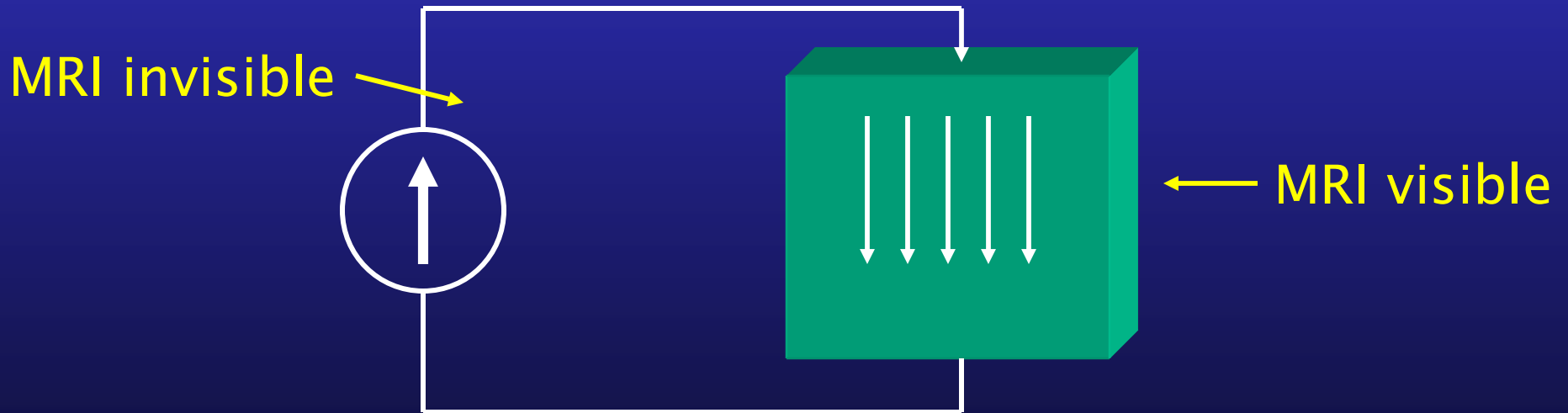
Map H_x, H_y by MRI, & integrate divergence terms along z .

How to approximate/estimate $c(x, y, z_0)$?

$\nabla \times J$ Can provide extra constraint

Biot-Savart Law

$$4\pi\vec{H}(r') = \int_{\vec{v}} \vec{J}(r) \times \nabla \frac{1}{|r' - r|} dv$$



Must integrate over ALL current carrying regions.

Can transverse B1 maps be used to estimate Bz?

$$4\pi\vec{H}(r') = \int_{\forall} (\nabla \times \vec{H}) \times \nabla \frac{1}{|r' - r|} dv$$

$$- \int_s (\vec{n} \times \vec{H}) \times \nabla \frac{1}{|r' - r|} ds - \int_s (\vec{n} \cdot \vec{H}) \nabla \frac{1}{|r' - r|} ds$$

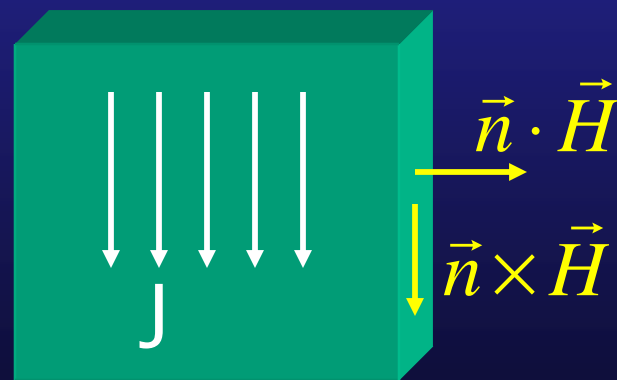
Exterior field surface integral correction

See Stratton, ch 4, ch 8.

Quasi-static,

Satisfies $\nabla' \cdot \vec{H}(r') = 0$

Need $\nabla \times J$



$$\vec{J} = (\sigma + j\omega\epsilon)\vec{E}$$

Full-Wave Source-free Volume

$$4\pi\vec{H}(r') = -\int_S (\vec{n} \cdot \vec{H}) \nabla \frac{e^{-jk|r'-r|}}{|r'-r|} ds - \int_S (\vec{n} \times \vec{J}_t) \frac{e^{-jk|r'-r|}}{|r'-r|} ds$$

$$- \int_S (\vec{n} \times \vec{H}) \times \nabla \frac{e^{-jk|r'-r|}}{|r'-r|} ds$$

$\vec{J}_t = (\sigma + j\omega\epsilon)\vec{E}_t$

Tangential H and E fully determine interior fields!



$$\vec{n} \times \vec{H}$$

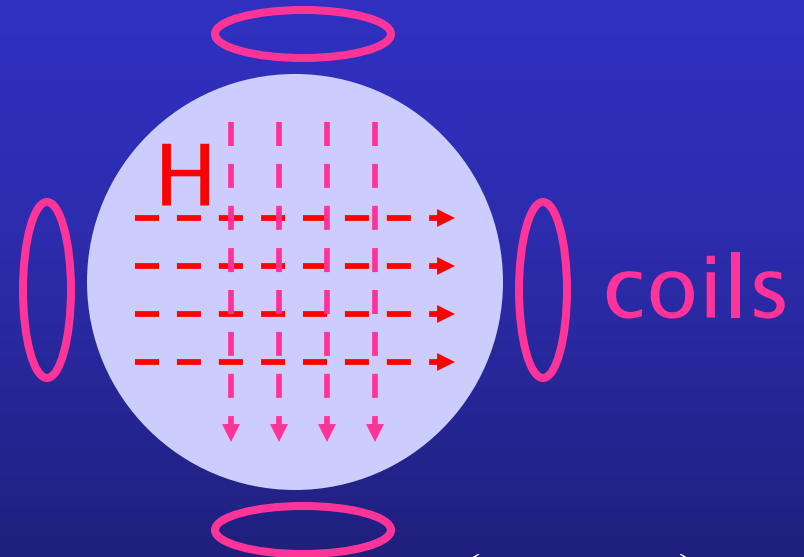
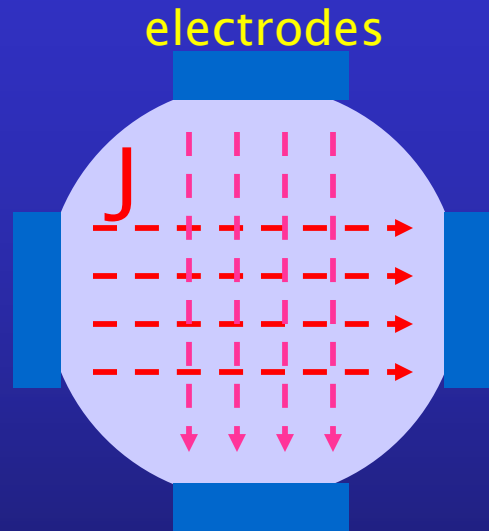
Electric Surface current K_e

$$\vec{n} \cdot \vec{H}$$

Magnetic Surface current K_m

$$\vec{n} \times \vec{E}$$

What about Admittivity Gradients: $\vec{J} \times \frac{\nabla(\sigma + j\omega\epsilon)}{(\sigma + j\omega\epsilon)}$



$$-\nabla^2 H_z = J \times \frac{\nabla \sigma}{\sigma} = \nabla V \times \nabla \sigma$$

Harmonic Bz Algorithm

Seo IEEE TBE, 50:1121, 2003,

Oh PMB 48:3101, 2003

$$\nabla^2 H_x = j\omega\mu\hat{\sigma}H_x + \left(J \times \frac{\nabla \hat{\sigma}}{\hat{\sigma}} \right)_x$$

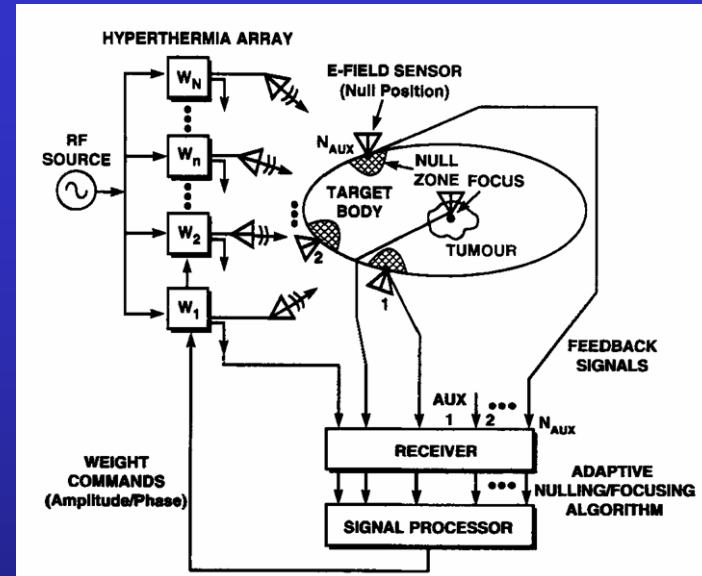
Zhang, IEEE TMI 29, 474, 2010.

Transverse Electric?

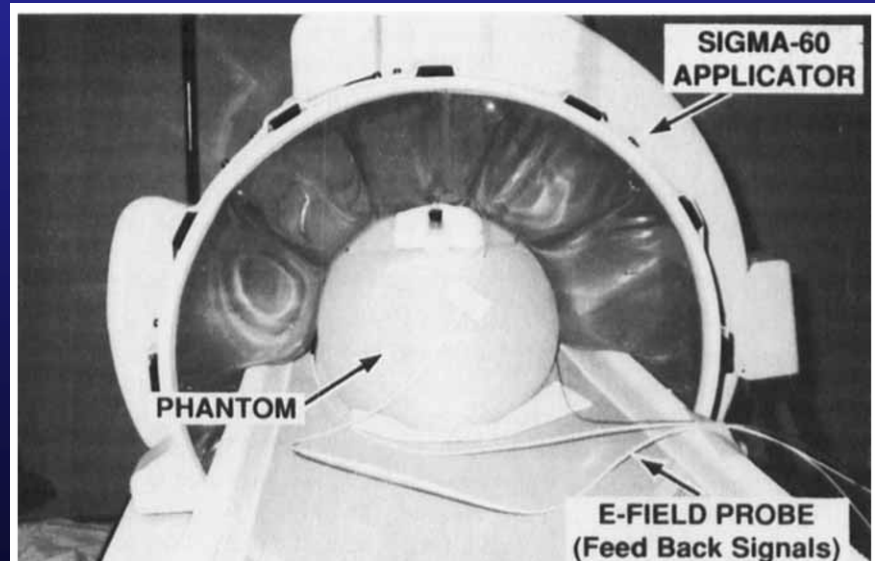
Transverse Magnetic?

Hyperthermia Systems

BSD-2000/3D/MRI

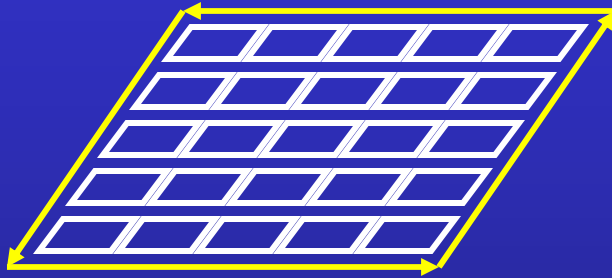


24-dipole Antennas, 12
Power Amplifiers



Fenn, Int. J Hyperthermia 10,189, 1994

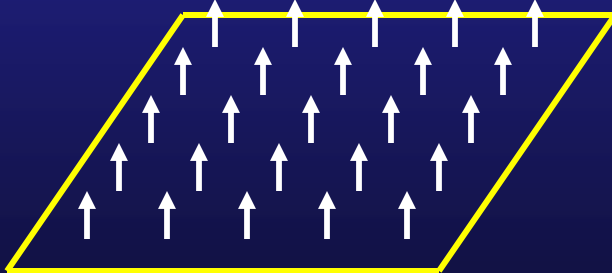
Coil



2D Magnetic dipole surface

$$J = \nabla \times M$$

$$J_m = j\omega\mu_0 M$$

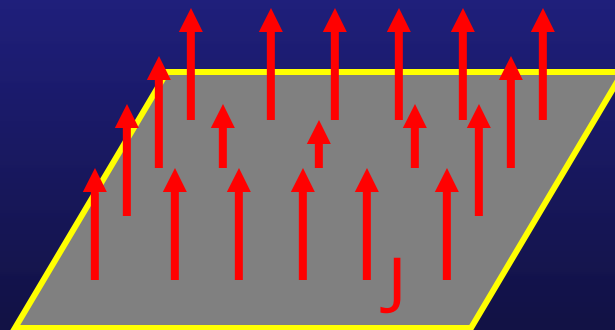


Magnetic current density normal to coil plane

Electrode

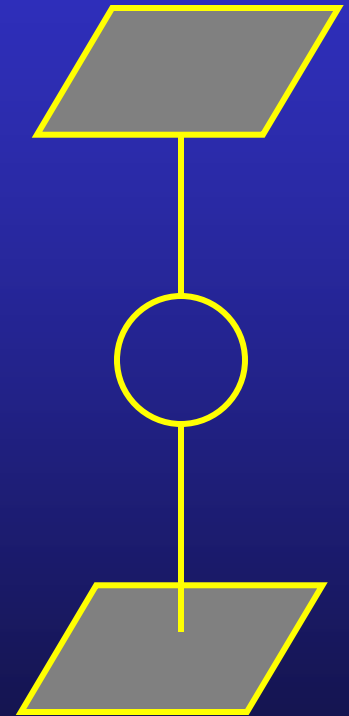


Perfect Electric Conductor



Electric current density normal to electrode plane

Antenna



Antenna

Summary

- § EPT methods use AFI/MTM, SE and GRE – no real B1 maps.
 - § Laplacian computation.
- § RF CDI creates conductivity contrast by injecting RF current & B1 mapping.
 - § Curl computation.
- § Integral equation, and multiple (array) transmit.
- § Coils and electrodes are equivalent to exciting by magnetic current sources & electric current sources.